PACIFIC CLIMATE IMPACTS CONSORTIUM

Climate Extremes in the Canadian Columbia Basin:

A Preliminary Assessment

19 August 2013

Trevor Q. Murdock

Stephen R. Sobie

Climate extremes in the Canadian Columbia Basin

Executive Summary v
Citation vi
About PCIC vi
Acknowledgements vi
1. Introduction 1
1.1. About CACCI 1
1.2. Analysis of climate extremes 1
1.3. Regional climate model projections of extremes 2
2. Indices of extremes 7
2.1. Extremes of interest 7
2.2. List of indices studied 8
Percentiles 8
Return periods 9
Simple temperature & precipitation indices 9
Complex parameters - CLIMDEX 10
Complex parameters – specialized 10
2.3. Discussion of indices selected 11
3. Historical simulations 12
3.1. Basin average 12
3.2. Seasons and sub-regions 18
3.3. Value-added 20
4. Future projections – results and discussion 26
Basin-average change in mean and variability 26
Ranges of change 27
4.1. Percentiles 30
4.2. Return periods 33
4.3. Simple temperature and precipitation indices: 35
4.4. Complex indices 38
Consecutive days CLIMDEX indices 38
Threshold CLIMDEX indices 39

Specialized complex indices 40
5. Summary 41
5.1. Temperature 41
5.2. Precipitation 41
5.3. Other extremes 42
5.4. Indices of interest 42
5.5. Uncertainty 42
References 44
Appendix 1: Results summary tables 47
Appendix 2: Table of RCM details 51
Appendix 3: Possible Future Work 52

Executive Summary

Since 2008, a number of communities in the Columbia Basin have undertaken climate change adaptation planning with the support of the Columbia Basin Trust. Most of these communities have requested more detailed information on potential changes in extreme weather and climate to inform their planning processes, but until now that information was not available in a regionally-detailed form. This report presents the findings of a preliminary investigation to address that gap. Regional projections of changes to indices of extremes are analysed for the Canadian portion of the Columbia Basin.

The report is the first such regional assessment of extremes by the Pacific Climate Impacts Consortium. The assessment uses simulations of past and future climate from Regional Climate Models to generate the analysis. Present-day climate simulated by Regional Climate Models[1] is first compared to observations. Good agreement with gridded observations in terms of seasonal and annual temperature and precipitation is found. The results from future projections are broadly as follows: considerable warming and more frequent occurrence of warm extremes, modest changes in wet precipitation extremes, and complicated changes in other indices.

All basin-average temperature extremes analyzed for this study are projected to increase by the 2050s compared to the 1971-2000 baseline. There is a range of projected change including instances of very little or no increase for certain indices at specific locations and times of year. At the warm end of the range, some simulations project dramatic changes such as over 3 times as many warm days, a 12°C increase in monthly maximum temperature (during May), less than half as many cold days, a 10-fold increase in the number of days during warm spells, and an 11-fold increase in the frequency of occurrence of 25-year record extremely hot days.

Projected changes in precipitation by the 2050s compared with the 1971-2000 baseline are broadly consistent with GCM projected decreases in summer precipitation and increases in other seasons. Over the region as a whole, extreme precipitation events (5-, 10-, and 25-year return periods) are projected to occur two to three times more frequently. While there is considerable variation in the pattern of projected precipitation changes within the basin, one of the more consistent results among models is the largest increases in precipitation extremes occurring in the Columbia Shuswap sub-region and smallest increases occurring in the Southern East Kootenay.

More complex indices of extremes are also considered. These variables depend on measures such as absolute thresholds or counting consecutive days and address important concerns such as drought and flood risk. Results for these complex indices are generally inconclusive; additional work, such as incorporating bias corrections or some form of downscaling to stations, would be required to assess them further.

Finally, the ensemble of eight RCM projections used here is relatively small. A comparison of the driving GCM temperature and precipitation over the region gives some confidence that this small ensemble captures a reasonable part of the range of plausible projections of regional change in most seasons, but care should be taken to interpret the ranges projected here as a preliminary assessment, to be refined in future with additional RCM runs and further analysis.

[1] From the North American Regional Climate Change Assessment Program (NARCCAP)

Citation

Murdock, T.Q., S.R. Sobie, 2013: *Climate Extremes in the Canadian Columbia Basin: A Preliminary Assessment.* Pacific Climate Impacts Consortium, University of Victoria, Victoria, BC, 52 pp.

About PCIC

The Pacific Climate Impacts Consortium is a regional climate service centre at the University of Victoria that provides practical information on the physical impacts of climate variability and change in the Pacific and Yukon Region of Canada. PCIC operates in collaboration with climate researchers and regional stakeholders on projects driven by user needs. For more information see http://pacificclimate.org.

Disclaimer

Acknowledgements

The authors are grateful to the vision of the Columbia Basin Trust and its employees in defining the project that led to the results reported on in this document, in particular Kindy Gosal, Ingrid Liepa, and Michelle Laurie. This work also would not have been possible without input during the project from a Project Advisory Group consisting of Greg Utzig, Dr. Mel Reasoner, Ingrid Liepa, Cindy Pearce, and Meredith Hamstead. The project also depended on teamwork internally within the Pacific Climate Impacts Consortium. We thank our colleagues for extremely valuable contributions: Hailey Eckstrand (mapping and analysis), James Hiebert and Dave Bronaugh (data management and indices scripts), Dr. Gerd Bürger (return periods), Dr. Francis Zwiers (project management and review), Dr. Dave Rodenhuis (project definition), and Cassbreea Dewis (administration). Finally, we appreciate two anonymous external reviews as well as reviews by Dr. Barbara Casati, Cindy Pearce and the Columbia Basin Trust climate change adaptation team: Ingrid Liepa, Jeff Zukiwsky, and Katherine Mahoney.

The CRCM data has been generated and supplied to the North American Regional Climate Change Assessment Program (NARCCAP) by Ouranos. We wish to thank Ouranos and NARCCAP for providing the data used in this paper. NARCCAP is funded by the National Science Foundation (NSF), the U.S. Department of Energy (DoE), the National Oceanic and Atmospheric Administration (NOAA), and the U.S. Environmental Protection Agency Office of Research and Development (EPA).

1. Introduction

This report is one in a series that provides information on climate change and its impacts in the Canadian Columbia River Basin. It documents the results of a year-long project to provide information on extremes for use in the Columbia Basin Trust's ongoing *Communities Adapting to Climate Changing Initiative* (CACCI).

The scope of this report is to provide an initial set of regional future projections of indices of climate extremes in the basin. First, some background on the indices selected is given in Section 2. This is followed in Section 3 by a basic assessment and discussion of the simulation of historical climate by Regional Climate Models. Results and discussion are presented in Section 4 and followed by a summary in Section 5. The summary includes a synthesis of the projected changes in the different types of indices (Section 5.4) and a description of five factors that contribute to addressing uncertainty (Section 5.5).

The report is fairly technical in nature and intended as a resource to inform further synthesis of results and to guide further work. More general information is available in other related reports on historical variability, trends, and future impacts (Murdock & Werner, 2011), impacts and adaptation literature review (Lane et al. 2010), and synthesis (Pearce 2011).

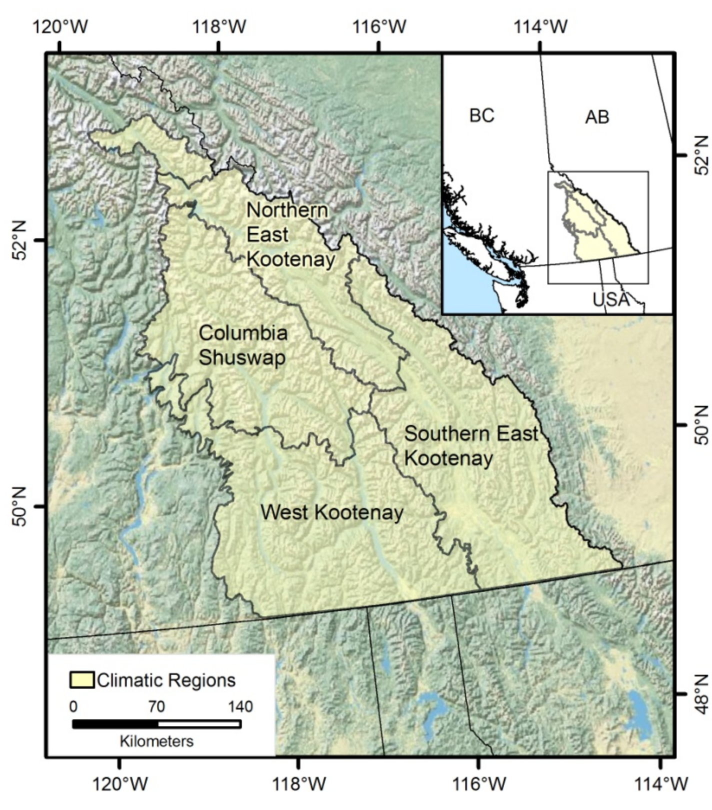

Figure 1: Study area: Canadian Columbia River Basin (light green) and climatic sub-regions: Columbia Shuswap, North East Kootenay, West Kootenay, and Southern East Kootenay based on local influences of climate on ecosystems (Greg Utzig, pers. comm.).

1.1. About CACCI

The *Communities Adapting to Climate Changing Initiative* (CACCI) is a Columbia Basin Trust initiative that seeks to increase the capacity of communities in the basin to adapt to climate change. Given the importance of understanding the possible range of future climate extremes when communities are planning for adaptation, this document provides information applicable to the entire region. The study area is shown in Figure 1.

1.2. Analysis of climate extremes

The Intergovernmental Panel on Climate Change (IPCC) report *Managing the risks of extreme events and disasters to advance climate change adaptation* (IPCC 2012) includes several global, continental, and sub-continental findings relevant to the region:

1. A changing climate leads to changes in the frequency, intensity, spatial extent, duration, and timing of extreme weather and climate events, and can result in unprecedented extreme weather and climate events.
2. It is very likely that there has been an overall decrease in the number of cold days and nights and an overall increase in the number of warm days and nights, on the global scale, i.e. for most land areas with sufficient data. It is likely that these changes have also occurred at the continental scale in North America. … In many (but not all) regions over the globe with sufficient data there is medium confidence that the length or number of warm spells, or heat waves, has increased.
3. It is virtually certain that increases in the frequency and magnitude of warm daily temperature extremes and decreases in cold extremes will occur in the 21^{st} century on the global scale. It is very likely that the length, frequency, and/or intensity of warm spells, or heat waves, will increase over most land areas. Based on the A1B and A2 emissions scenarios, a 1 in 20 year hottest day is likely to become a 1 in 2 year event by the end of the 21^{st} century in most regions except in the high latitudes of the Northern Hemisphere where it is likely to become a 1 in 5 year event.
4. It is likely that the frequency of heavy precipitation or the proportion of total rainfall from heavy falls will increase in the 21^{st} century over many areas of the globe.
5. While there is low confidence in the detailed geographical projections of extra-tropical cyclone activity, there is medium confidence in a projected poleward shift of extra-tropical storm tracks.
6. There is medium confidence that droughts will intensify in the 21^{st} century in some seasons and areas, due to reduced precipitation and/or increased evapotranspiration.

1.3. Regional climate model projections of extremes

Some aspects of adaptation planning may be informed by coarse resolution information about changes to future climate, such as changes in 30-year annual or seasonally averaged quantities that are obtained from Global Climate Models (GCMs). However, progress towards the implementation of, in some cases costly, adaptation measures often requires more detailed and regionally specific information. While analysis of regional measures of extremes is an emerging activity, it is required to take adaptation to the next stage (Zhang et al. 2008).

The findings about future projections summarized in section 1.2 are based on results of GCMs. Our interpretation of GCM projections is restricted to sub-continental scales because of their coarse spatial resolution. Projected change in future temperature extremes (item 3 above) based on GCMs is illustrated in Figure 2 for the globe (Kharin et al. 2007). The waiting time for the historical (1990) 20-year return period daytime high temperature (T_{max}) in future (2046-2065) shows a considerable reduction to a waiting time of only 2 to 3 years by the middle of the century in much of Western North America, that is 7 to 10 times more frequent than in the late 20^{th} century. The 20-year return period daily precipitation event for Western North America (item 4 above) is projected to occur every 10 to 15 years (IPCC 2012).

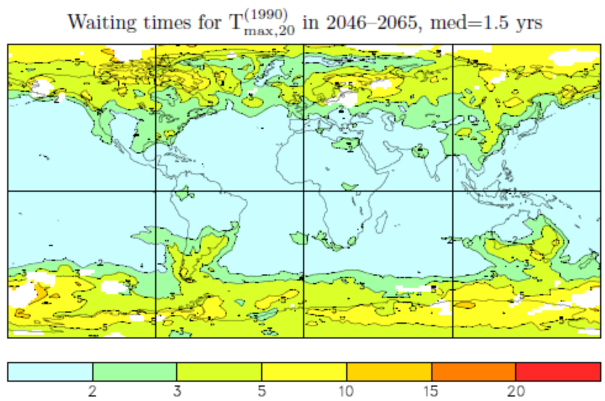

Figure 2: Change in 1990 20-yr return period of daytime high temperature (Tmax) from an ensemble of GCMs. Source: (Kharin et al. 2007).

One way to increase the spatial resolution of GCM results, to make them applicable to smaller regions such as the basin, is to use Regional Climate Models (RCMs) to dynamically downscale GCM projections. However, fewer projections from RCMs are available than from GCMs and the first inter-comparison of RCM results for North America, the *North American Regional Climate Change Assessment Program* (NARCCAP) has only recently started providing results. We have used eight NARCCAP projections driven by four different GCM projections (Table 4 in Section 4 provides a list of RCMs and driving GCMs). Each RCM simulation of past climate in the basin is compared to observations (see Section 3). Throughout this report, we will refer to a single future projection as a "run" rather than a "model" because some of the RCMs are driven by multiple GCMs so a run represents not only the RCM but also the driving model conditions.

A key strength of GCMs is the large number of simulations available from them, which allows for exploration of uncertainty. For example, the boxplot in Figure 3 shows the range of projected climate change according to the four individual GCM projections[i] that drive the NARCCAP RCMs used in this report and a larger ensemble (PCIC30[ii]). The range of projected change widens throughout the 21st century, a pattern that holds true for each season (Figure 4).

The PCIC30 ensemble shown in Figure 4 tends to project slightly larger increases in summer temperature in future than other seasons. This set of 30 projections includes 15 different GCMs and was defined prior to the selection of NARCCAP driving GCM runs. Two of the four NARCCAP driving GCMs are also members of the PCIC30 ensemble (CGCM3 and HadCM3) but different runs (run 5 in both cases) are used than in PCIC30 (all run 1). Projected changes to precipitation (Figure 5) depend highly on the season; increases in precipitation are projected by most models in all seasons except summer, where precipitation is projected to decrease according to most GCMs.

It is apparent from Figures 3 to 5 that the four individual projections used to drive the RCMs represent in some cases a narrower range of uncertainty than the wider PCIC30 range, particularly for temperature. On the other hand, for precipitation the range of the four GCM projections used to drive RCMs is wider than the range from the PCIC30 ensemble in some cases: on the high side in all seasons and on the low side in summer and fall. Note that CGCM3 and CCSM each drive three RCM runs while HadCM3 and GFDLCM2.1 each drive only one RCM run in our ensemble. Thus, the CGCM3 and CCSM anomalies are representative of the bulk of the ensemble.

[i] CGCM3 A2 run 5, CCSM30 A2 run 5, HadCM3 A2 run N (for NARCCAP), GFDL CM21 A2 run 5

[ii] The PCIC30 ensemble is run 1 of B1 and A2 from each of the following GCMs: BCCR BCM20, CCCMA CGCM3, CNRM CM3, CSIRO MK30, GFDL CM20, GFDL CM21, GISS ER, INM CM30, IPSL CM4, MIROC32 MEDRES, MIUB ECHOG, MPI ECHAM5, MRI CGCM232A, NCAR CCSM30, UKMO HADCM3

The projected range of change based on the eight RCM runs thus generally represents a subset of the range of plausible futures represented by ensembles that include many models and multiple emissions scenarios. These differences between the RCM ensemble and the wider ensemble are important to consider when using the projections in this report.

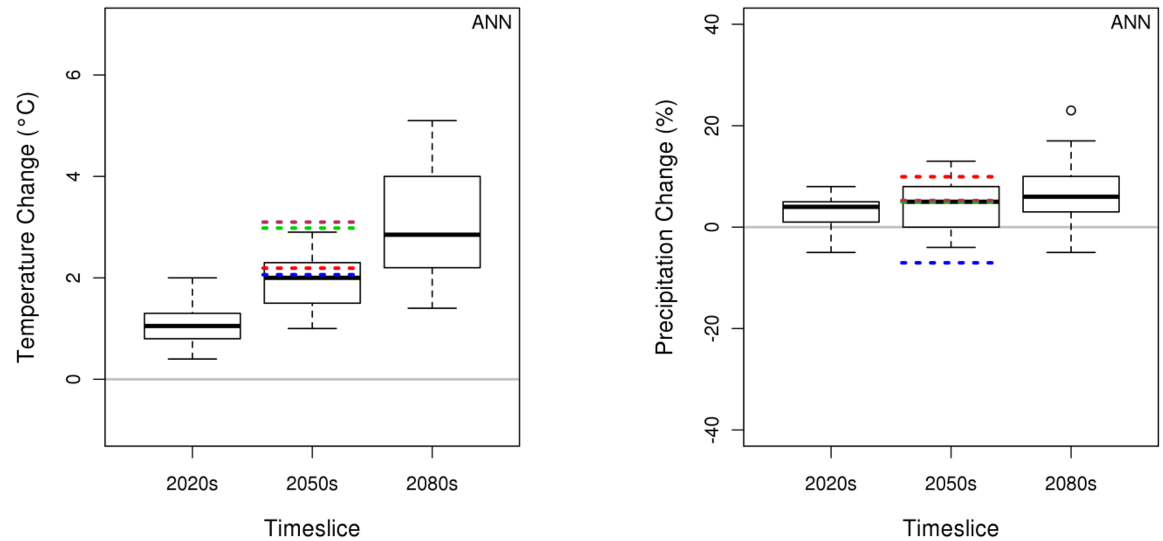

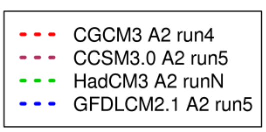

Figure 3: Annual mean temperature (left) and precipitation (right) change projected by the PCIC30 ensemble for the Columbia Basin region. The heavy line shows the median, the box shows the 25th to 75th percentile, and the whiskers represent 1.5 times the inter-quartile range (IQR) from the median. Runs further from the median than the IQR are shown as circles. The dashed coloured lines show the change projected by GCM runs used to drive the NARCCAP RCMs. See text (Section 1.2) for differences in region and baseline definition between boxes and coloured lines.

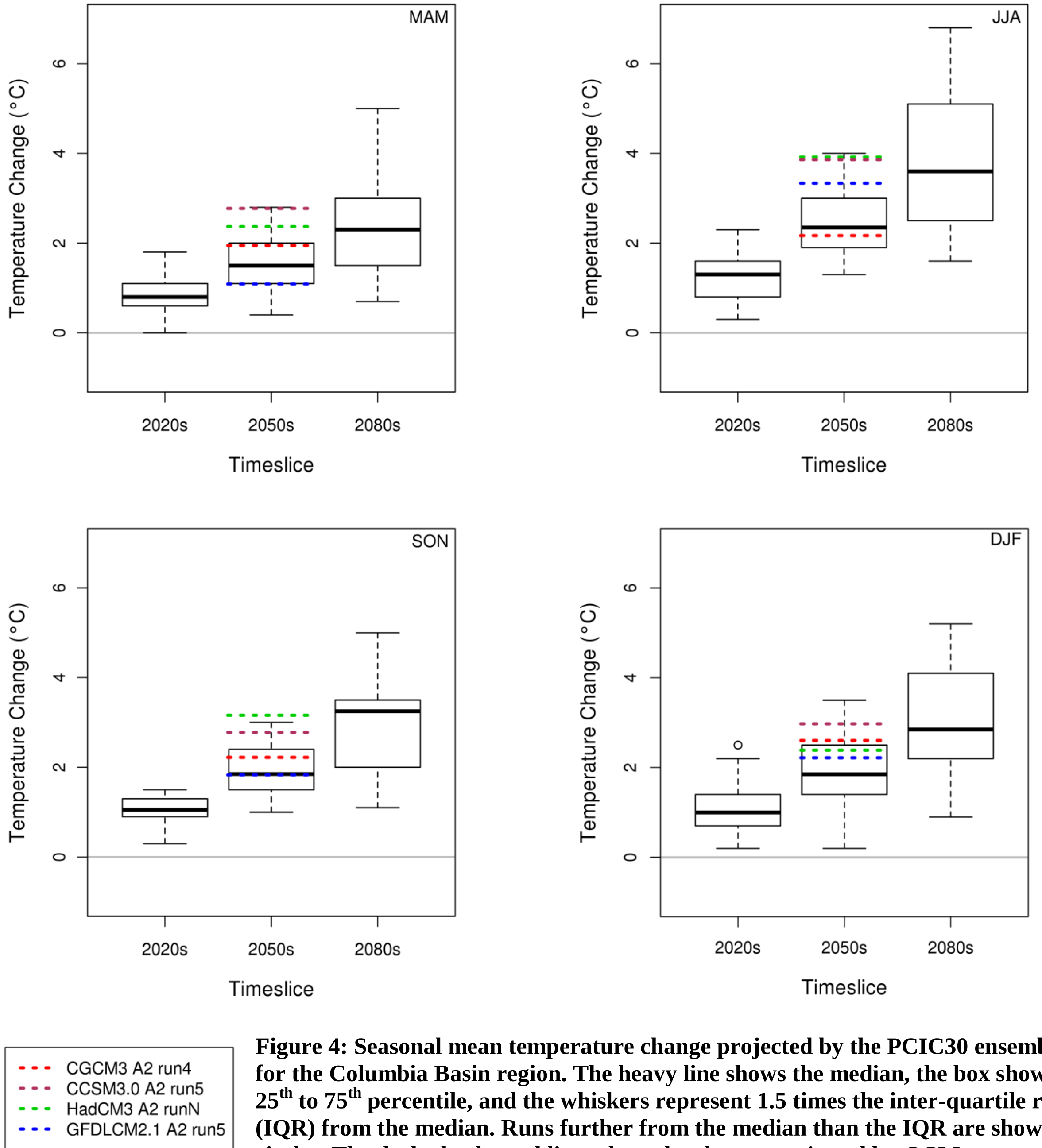

Figure 4: Seasonal mean temperature change projected by the PCIC30 ensemble for the Columbia Basin region. The heavy line shows the median, the box shows the 25th to 75th percentile, and the whiskers represent 1.5 times the inter-quartile range (IQR) from the median. Runs further from the median than the IQR are shown as circles. The dashed coloured lines show the change projected by GCM runs used to drive the NARCCAP RCMs. See text (Section 1.2) for differences in region and baseline definition between boxes and coloured lines.

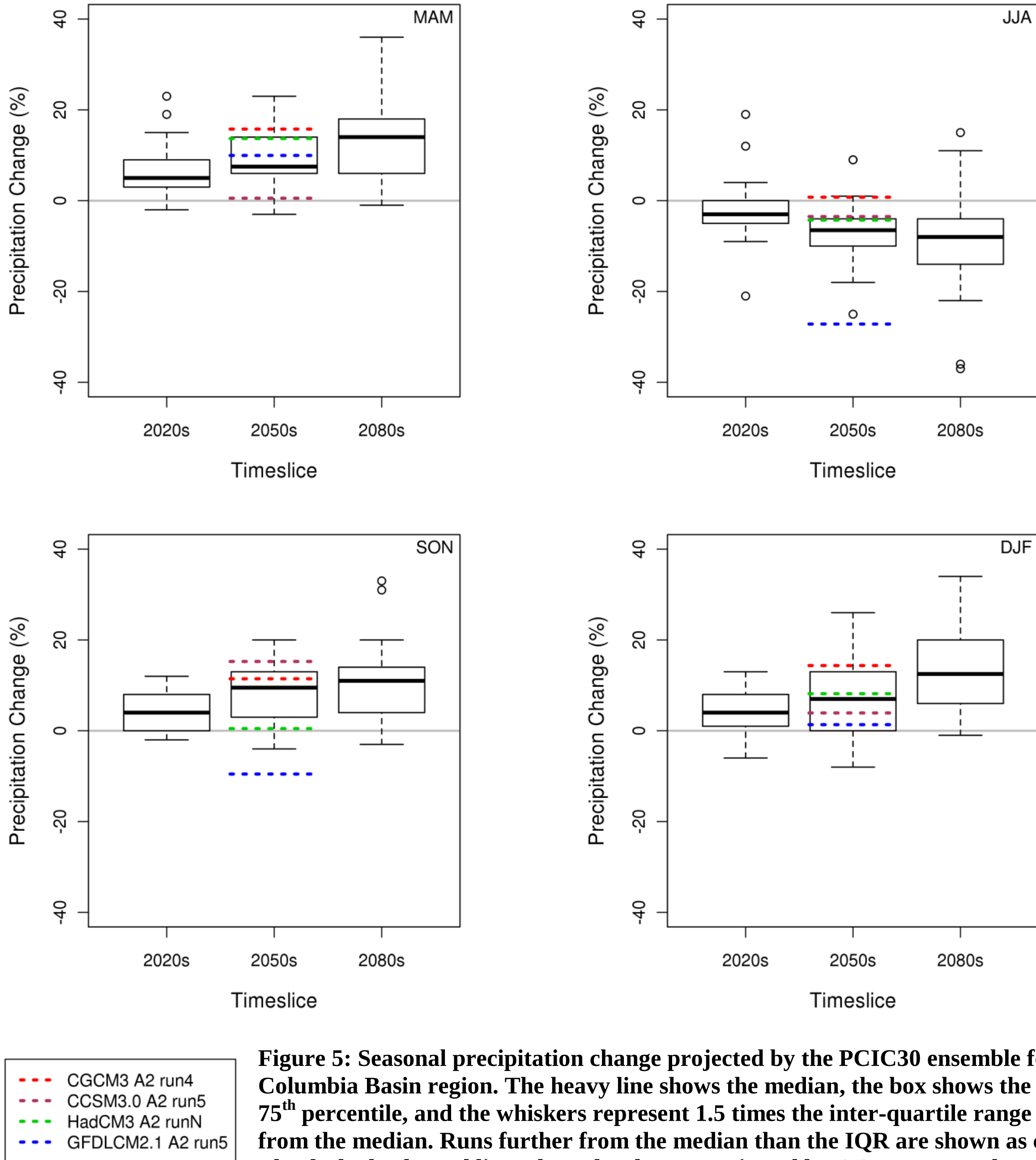

Figure 5: Seasonal precipitation change projected by the PCIC30 ensemble for the Columbia Basin region. The heavy line shows the median, the box shows the 25th to 75th percentile, and the whiskers represent 1.5 times the inter-quartile range (IQR) from the median. Runs further from the median than the IQR are shown as circles. The dashed coloured lines show the change projected by GCM runs used to drive the NARCCAP RCMs. See text (Section 1.2) for differences in region and baseline definition between boxes and coloured lines.

2. Indices of extremes

The list of parameters considered in this report was determined by seeking a balance between indices that have been studied elsewhere regionally (e.g., Goodess et al. 2005), feasibility of computing them, and perceived usefulness to adaptation planning. Input on extremes of interest was provided by a Project Advisory Group[iii] (Section 2.1). We also drew upon recent experience gained by PCIC with statistical downscaling of indices of extremes to specific sites, including a stormwater vulnerability assessment within the basin (Castlegar 2011). The resulting set of indices (Section 2.2) is the full CLIMDEX set of standard indices and return periods of climate extremes defined by the Expert Team on Climate Change Detection and Indices (Peterson et al. 2001; Zhang et al. 2011) as well as a small number of specialized indices. The climdex indices were analysed using the climdex.pcic R-package[iv] developed at PCIC.

2.1. Extremes of interest

The Project Advisory Group (PAG) provided a list of desired types of indices for extremes along with comments and rationale on why they would be useful. This input was used to assist the interpretation and summary of results. The PAG's input on seven categories of indices is summarized below. This list is based on the group's expert opinions and perceptions of climate change vulnerabilities for the region and is not constrained by availability of data or resources.

1. The PAG indicated that **drought** is important because it can result in a wide range of further impacts on sectors such as agriculture, municipal water use, water quality, fisheries, and other ecosystem impacts. Assessing meteorological drought requires only information about (lack of) precipitation, whereas assessing agricultural or hydrological drought requires, at a minimum, information about simultaneous occurrence of hot temperatures with lack of precipitation.
2. **Extreme fire weather** is similar to drought in its dependence on both hot temperatures and lack of precipitation. The PAG noted that relationships between climate and historic area burned in the basin appear to be associated with high maximum temperatures for July/August throughout the area as well as spring maximum temperatures and June precipitation in the northern basin, with June/July/August precipitation and seasonal climatic moisture deficit playing a role in the Mid and Southern portions of the region.
3. The PAG indicated that an index of **late spring frosts** would ideally count the number of days below freezing after the accumulation of enough degree days over a threshold such as 5°C to bring about bud burst or the number of days below a threshold temperature in May and June, as the PAG indicated these months are the likely times for killer frosts to occur.
4. Similarly, the PAG's ideal index of **ground penetrating frost** would count days below 0°C when there is little or no snow on the ground such as a combination of snow depth and cold spells.

[iii] The Project Advisory Team consisted of Greg Utzig, Mel Reasoner, Ingrid Liepa, Cindy Pearce, Meredith Hamstead, and Michelle Laurie.

[iv] http://cran.r-project.org/web/packages/climdex.pcic/index.html

5. **High intensity precipitation** in the basin that was of most interest to the PAG was large accumulations of precipitation during periods of several days as it was suggested that this would usually be necessary to create sufficient infiltration to initiate landslides and/or generate sufficient runoff for serious flood events.
6. Although **stream low flow events** would be related to drought, the PAG indicated that annual events of concern could also be expected to result from a combination of one or more of: a) low snow accumulation in the previous winter, b) early spring snowmelt and/or c) severe spring/summer drought.
7. The PAG expressed interest in **extreme windstorm events**, including information on projected changes to prevailing wind direction and frequency of occurrence of high wind speeds.

2.2. List of indices studied

The list of 54 indices below includes all parameters analyzed for this project. Some variables are available on an annual, seasonal, and monthly basis. In addition to the indices listed below, projected change in 30-year average temperature and precipitation were investigated to provide context to projected changes in indices of extremes.

Percentiles

Temperature-related percentiles include the four indices listed in bullets below. Each of these was computed on an annual, seasonal, and monthly basis. Note that 10p and 90p refer to the 10th and 90th percentiles of both daytime high (maximum) and nighttime low (minimum) temperatures for each day of the year (using a 5-day window centered on that day to get a larger sample size) during the 1971-2000 baseline. Thus, these variables measure warm or cold relative to the day of the year rather than using a constant threshold throughout the year. These parameters measure how often temperatures exceed the 10p and 90p thresholds – they are measures of the frequency of occurrence of such events.

- Cool nights - TN10p: occurrence of minimum temperature < 10p
- Warm days - TX90p: occurrence of maximum temperature > 90p
- Cool days - TX10p: occurrence of maximum temperature < 10p
- Warm nights - TN90p: occurrence of minimum temperature > 90p

Two precipitation-related percetntile indices differ from temperature in that they are not measures of frequency of occurrence but rather the annual *amount* of total precipitation that occurs during the events when precipitation exceeds the 95th or 99th percentile of all rain days (regardless of the day of the year in which they occur). Thus, these measures indicate how much of the total precipitation in a year falls during these wet events, which is a combination of *both* how often events occur that exceed baseline 95th and 99th percentile thresholds *and* the size of these events.

- Very wet day precipitation - R95pTOT: annual total precipitation when > 95p
- Extremely wet day precipitation - R99pTOT: annual total precipitation when > 99p

Return periods

Changes in return periods are investigated to estimate the change in extremely rare events. The return periods correspond to the maximum (for right side) or minimum (left side) events so rare that they are expected to happen only once every 5, 10, or 25 years on average (see Table 1). These may also be interpreted as the events with a 20%, 10%, and 4% chance of occurring each year, respectively. Longer (50-, 100-, and 200-year) return periods were also requested but the time series available from the RCMs are insufficient (30 years) for robust analysis of these longer time frames. Methods exist to overcome this limitation at the expense of spatial resolution, a possible option for future work (van den Brink & Können 2011).

Return periods for precipitation events were estimated for both daily and 3-hourly durations. The duration refers to the sampling interval for which accumulations are reported (either once a day or once every 3 hours). Both durations are considerably larger than the minimum time step used in the models (typically 15-20 minutes) so temporal resolution is sufficient for their computation. Daily return periods have been studied with GCMs and were computed for comparison with such previous work. The 3-hourly return periods were also calculated for precipitation as they represent the highest time resolution at which archived data was available. Despite the focus on multi-day events, the PAG was also interested in changes to the maximum precipitation rate experience during an event, which the 3-hourly resolution more closely represents by avoiding averaging over a 24-hour period. The shorter duration might be particularly important to capture changes in extreme summer precipitation which tends to feature intense convective storms.

Return periods were estimated by fitting the annual maxima of RCM simulated values to the Generalized Extreme Value (GEV) distribution. This was done for both the historical and future periods separately. The GEV is a probability distribution that can be used to approximate the actual distribution of annual maxima using only three parameters (called the scale, shape, and location parameters). This is similar to how a normally distributed function can be represented by only its mean and standard deviation. The GEV distribution originates in statistical extreme value theory and works well in many practical applications. By approximating the distribution of annual maxima with the GEV, we can then use known properties of the GEV distribution to estimate return periods. The GEV analysis was performed using the fExtremes package for the R software programming language which uses the method of L-moments (Hosking 1985) and uncertainty was assessed based on the standard errors and confidence intervals of estimates of the three GEV parameters.

Table 1: Return periods analyzed

Variable	Return period	Duration	Side
Temperature	5, 10, 25	Daily	Right (warm), left (cold)
Precipitation	5, 10, 25	3 hourly, daily	Right (wet)
Snow depth	5, 10, 25	Daily	Right (deep)

Simple temperature & precipitation indices

Simple temperature related indices are those from CLIMDEX that do not depend on absolute thresholds, consecutive days, or interactions between temperature and precipitation. Each of these parameters was analyzed on an annual, seasonal, and monthly basis.

- Daily temperature range - DTR: diurnal temperature range
- Hottest day - TXx: monthly maximum value of daily maximum temperature
- Hottest night - TNx: monthly maximum value of daily minimum temperature
- Coldest day - TXn: monthly minimum value of daily maximum temperature
- Coldest night - TNn: monthly minimum value of daily minimum temperature
- Heaviest precipitation day - RX1day: monthly maximum 1-day precipitation
- Heaviest 5-day precipitation - RX5day: monthly maximum consecutive 5-day precipitation

The only precipitation related index from CLIMDEX, other than percentiles, that does not depend on absolute thresholds, consecutive days, or interactions with temperature is RX1day. The so-called simple (daily) precipitation index (SDII) – the average amount of precipitation that falls on wet days is included in the list of complex parameters below because it depends on a threshold to determine wet days. Conversely, RX5day is included here despite the consecutive days to keep it with the related RX1day.

Complex parameters - CLIMDEX

The following indices from CLIMDEX depend on consecutive days, absolute thresholds, or both. The definition of each of these parameters is given with the results (Section 4). See also www.climdex.org for definitions.

- WSDI: warm spell duration index
- CSDI: cold spell duration index
- CDD: maximum length of dry spell
- CWD: maximum length of wet spell
- GSL: growing season length
- FD: number of frost free days
- SU: number of summer days
- ID: number of icing days
- TR: number of tropical nights
- PRCPTOT: annual total precipitation in wet days
- SDII: simple precipitation intensity index
- R10mm: annual count of days when precipitation >= 10mm
- R20mm: annual count of days when precipitation >= 20mm

Complex parameters – specialized

Four custom-defined indices that are expected to be specifically relevant in the basin were analyzed. These were based on experience from recent case studies analyzing climate indices at site-specific basis, and adjusted based on feedback from the PAG. Each one depends on absolute thresholds, and three depend on both temperature and precipitation. Note that the purpose of these was exploratory – to investigate whether projections of such complex indices can be feasibly analysed using (non bias-corrected) RCM simulations. These four additional indices are not able to address all of the gaps between the extremes of interest listed in Section 2.1 and the suite of indices assessed (see discussion in Section 2.3).

- Freeze thaw cycles: night-time low < 0°C and day-time high > 0°C
- Rain on frozen ground: precipitation > 6 mm when no snow on ground and temperature < 0°C
- Rain on snow: snow pack > 10 mm, precipitation > 30 mm, and temperature > 0°C
- Rapid snow melt: snow melt > 10 cm in 3 hours

2.3. Discussion of indices selected

Some of the indices listed in Section 2.2 correspond directly to the extremes of interest described in Section 2.1. In particular, annual maximum 1-day or 5-day precipitation (RX1day and RX5day), and precipitation return periods each correspond directly to the high intensity precipitation information requested. Rain on snow and very wet precipitation (R95pTOT and R99pTOT) are also relevant.

The remaining categories are addressed less directly. For this reason the PAG considered the percentile indices as particularly useful because they indicate the general changes that might be expected to occur in moderate extremes. As such, changes in percentiles may be indicative of changes in other infrequent but not extremely rare events that are not directly addressed at this time. One of the biggest advantages of the percentile variables is that they are relative amounts. This makes them less influenced by model bias than absolute thresholds, and facilitates comparison of the results between different models. The percentile variables are also particularly appropriate for analysis of moderate extremes in a region such as the basin with complex topography, because the definition of warm, cool, and wet are relative to the distributions of temperature and precipitation at each individual grid box (Zhang et al. 2011).

Drought and extreme fire weather are addressed in part by warm spells (WSDI) and consecutive dry days (CDD), but information on their simultaneous occurrence is needed. Initial investigations took place into standard drought indices (van der Kamp et al. 2011) and an extreme fire weather index (van der Kamp & Bürger 2011) in the basin, in parallel to the work conducted here. Results indicate that an extension of this work using drought and fire weather indices is possible.

Although none of the indices address the late spring frosts directly, freezing and ice days (FD, ID) and freeze thaw cycles are relevant. Similarly, ground penetrating frost is influenced by both snow depth and cold spells (CSDI).

Stream low flow events are not directly addressed by the indices here and would require hydrological modelling to assess, such as work recently completed for the basin (Zwiers et al. 2011) and then applied to smaller watershed scales.

Although many of the extremes of interest are not directly addressed, the large list of indices considered are able to inform many of the areas of concern indirectly, as summarized in Section 5.4.

3. Historical simulations

Before considering future projections from RCMs, we first assess their historical skill using reanalysis-driven RCM simulations. A reanalysis is a gridded representation of the historical climate based on historical observations that have been "assimilated" into a global weather forecast model run in a hindcast mode. In the reanalysis-driven runs, we can compare individual years and seasons to the driving reanalysis and to observations for that year. The historical RCM simulations are virtually independent of local observations at the surface because the RCMs are driven only at the boundary of the domain by the reanalysis and in two cases (ECP2 and CRCM3) at coarse scales in the upper level atmosphere (called interior nudging).

To conduct a basic evaluation of how RCMs reproduce the climate of the basin, each of the six NARCCAP RCMs were compared to observed basin-average temperature and precipitation (Figure 6). Since we are comparing climate data at several different resolutions (Table 2), we have used area-weighted averages for all regional averages. For example, if a grid box has 12% overlap with the region boundary (see Figure 1), its value will be given 12% of the weight that is given to grid boxes that fall entirely within the region. We have not investigated historical skill for any of the indices directly, nor any measurement of daily values; we have assessed only the ability of the RCMs to reproduce seasonal and annual temperature and precipitation in the region.

Table 2: Observed datasets compared to NARCCAP NCEP2 driven historical simulations

Dataset	Full name	Resolution	Source
Stations	n/a	n/a	Environment Canada
CANGRD	CANGRID	50 km	(Zhang et al. 2000)
CRU	Climate Research Unit TS2.0	0.5° (~55 km)	(Mitchell & Jones 2005)
NARR	North American Regional Reanalysis	32 km	(Mesinger et al. 2005)
ANUSPLIN	Canadian Forest Service ANUSPLIN	10 km	(McKenney et al. 2006)
ANUSPLIN-PCIC	Canadian Forest Service ANUSPLIN for PCIC	1/16° (~7 km)	Custom interpolation for PCIC
UDEL	University of Delaware	0.5° (~55 km)	http://climate.geog.udel.edu/~climate/
VIC-PCIC	Variable Infiltration Capacity model driving data	1/16° (~7 km)	PCIC
NCEP2	National Centers for Environmental Prediction 2	T62 (~210 km)	(Kalnay et al. 1996; Kistler et al. 2001)

3.1. Basin average

First, we consider the annual average temperature for the basin (Figure 6 top panel). The stations stand out as warmer than all of the RCMs, but also warmer than all of the gridded observations. Since stations tend to be clustered in warmer valley bottoms while gridded observations include some form of elevation-based bias correction, we will compare RCMs to gridded observations rather than stations. Note that the data sets listed in Table 2 differ in more ways than resolution alone and an in depth comparison of the relative strengths and weaknesses is beyond the scope of this report. In Figures 6 and 7 we compare a range of observations to the spread of results from the RCM simulations. However, we also select a single dataset as a standard for comparison so that we can compare the different RCMs to a common historical dataset. We choose CANGRID for this purpose because its resolution is a near match to the RCMs themselves, its representation of elevation is best of the historical datasets (as shown in Figure 8 and related discussion in Section 3.1), and it has been used extensively for climate analysis in the region.

One simulation (HRM3) is considerably warmer than CANGRID by (2.7°C). Another simulation (CRCM) differs by 3.0°C from CANGRID, in this case with a cold bias. The rest of the RCMs are slightly colder than gridded observations, by an amount that is comparable to the spread between gridded observations themselves, and are is closer to gridded observations than NCEP2.

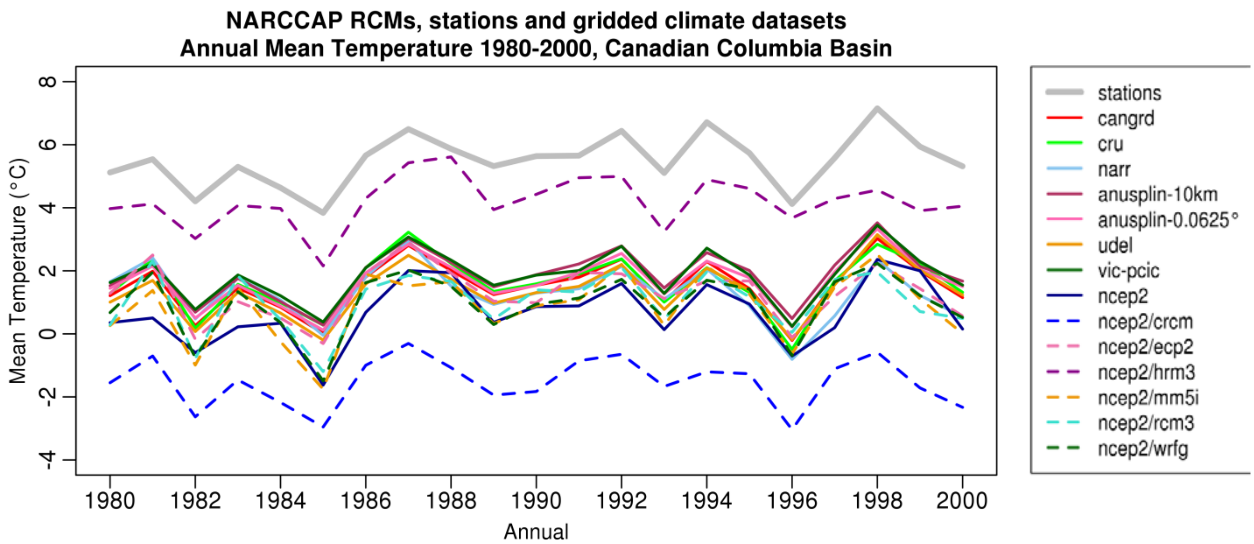

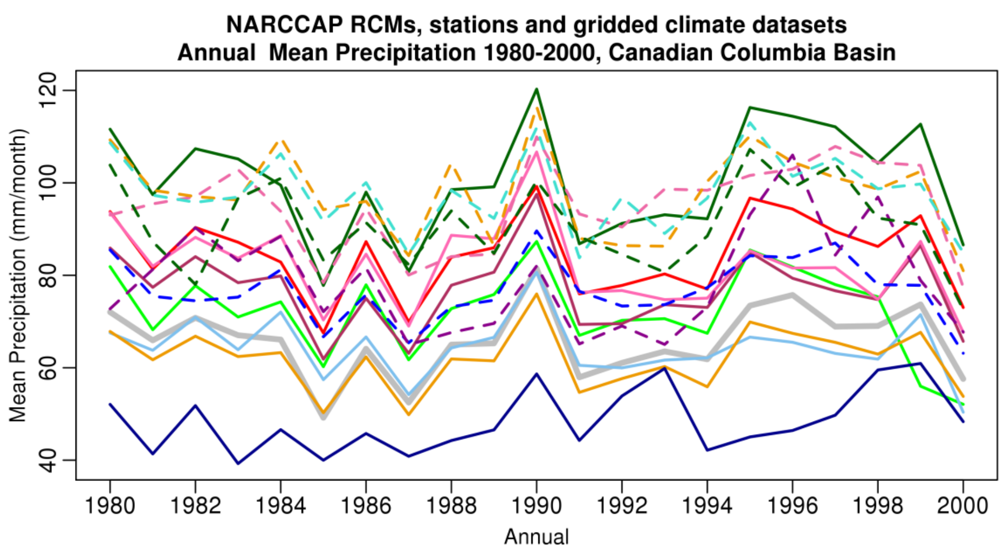

Figure 6: Annual temperature (upper panel) and precipitation (lower panel) for the basin as simulated by NCEP2-driven NARCCAP RCMs (dashed lines) and from gridded and station observations (solid lines). See Table 2 for sources of observed datasets.

Simulated historical precipitation by RCMs (Figure 6 bottom panel) varies by a factor of at least two. However, there is also little agreement between the observational datasets; that of precipitation among the different gridded observational datasets is even wider than the range of the models. In addition, comparison of RCM simulated precipitation to observations is complicated by the fact that the RCMs represent area averages but observations are based on point measurements, and precipitation is not spatially uniform (Klein Tank et al. 2009). In light of the spread of observational estimates of precipitation, the range of simulated RCM precipitation appears to agree fairly well with gridded observations overall, within 13 mm/month of CANGRID annual precipitation in all cases. Where differences occur, the RCMs tend to be on the wetter side of most gridded observations. The average of stations differs from the gridded precipitation observations due also to their primary location being in valley bottoms and the presence of bias corrections in the gridded datasets. NCEP2 precipitation is roughly half of most gridded observations, and even considerably less than station averaged precipitation. Note that precipitation observations are not assimilated in NCEP2; precipitation is considered a "type C" reanalysis variable, which means that it is determined primarily by the weather forecasting model used in NCEP2 rather than the assimilated observations (Kalnay et al., 1996).

Compared to CANGRID, we find that NCEP2 has a larger cold bias than all but the CRCM and a dry bias that is much larger than any of the RCMs (Figure 6). We consider this reduction in bias compared to their coarse resolution driving data (NCEP2) as part of the value added by the higher resolution of the RCMs.

This reduced historical bias is encouraging, but it is not sufficient to guarantee that future projections will be free of bias. We cannot directly assess skill of future projections, but we can get one step closer by considering the year-to-year response within the historical simulation. We do so by removing the 1980-2000 average from each record. This leaves a time series of annual anomalies from each record's average (Figure 7). Excellent agreement between the RCMs and observations indicates that most of the differences in Figure 6 between RCMs and gridded observations represent relatively constant biases. This is true even of HRM3 and CRCM temperature. Although simulated precipitation anomalies visually do not appear to follow observations as closely as temperature, the spread is similar to the spread of observed anomalies in most years. In general, the RCMs appear to capture larger annual precipitation anomalies more effectively than moderate anomalies (Figure 7 lower panel). For the majority of the indices of extremes studied here, capturing these smaller anomalies is less important than the larger anomalies.

These conclusions, which are based on visual inspection of Figures 6 and 7, are supported by basic measures of skill. The records of each NCEP2 driven RCM simulation and NCEP2 itself are compared to the CANGRID gridded dataset in Table 3. The bias reported is the difference between each record's 1980-2000 average and that of CANGRID. Root Mean Square Error (RMSE) is given for the bias corrected anomalies (as in Figure 7) from each record's baseline (see Equation 1). Correlations between the two datasets show that most RCMs perform as well as or better than NCEP2 in summer and similar to NCEP2 in other seasons. CRCM temperature anomalies exhibit the best correlation and RMSE despite having the largest bias. This result shows that high bias does not necessarily lead to poor skill. This gives some confidence in RCM future projections, which are given as changes from model simulated baseline to projected future. Indices based on absolute thresholds may still be considerably influenced by historical bias, however. Overall, the model with least skill across all seasons and measures is HRM3.

$$(1)\qquad RMSE = \left[\sum_{year=1980}^{2000} \left(X'_{\text{year,RCM}} - X'_{\text{year,CANGRID}}\right)^2\right]^{\frac{1}{2}}$$

$$where\ X'_{\text{year}} = X_{\text{year}} - X_{\text{avg}};\ X_{\text{avg}} = 1980 - 2000 \text{ baseline average}; X = \text{temperature or precipitation}$$

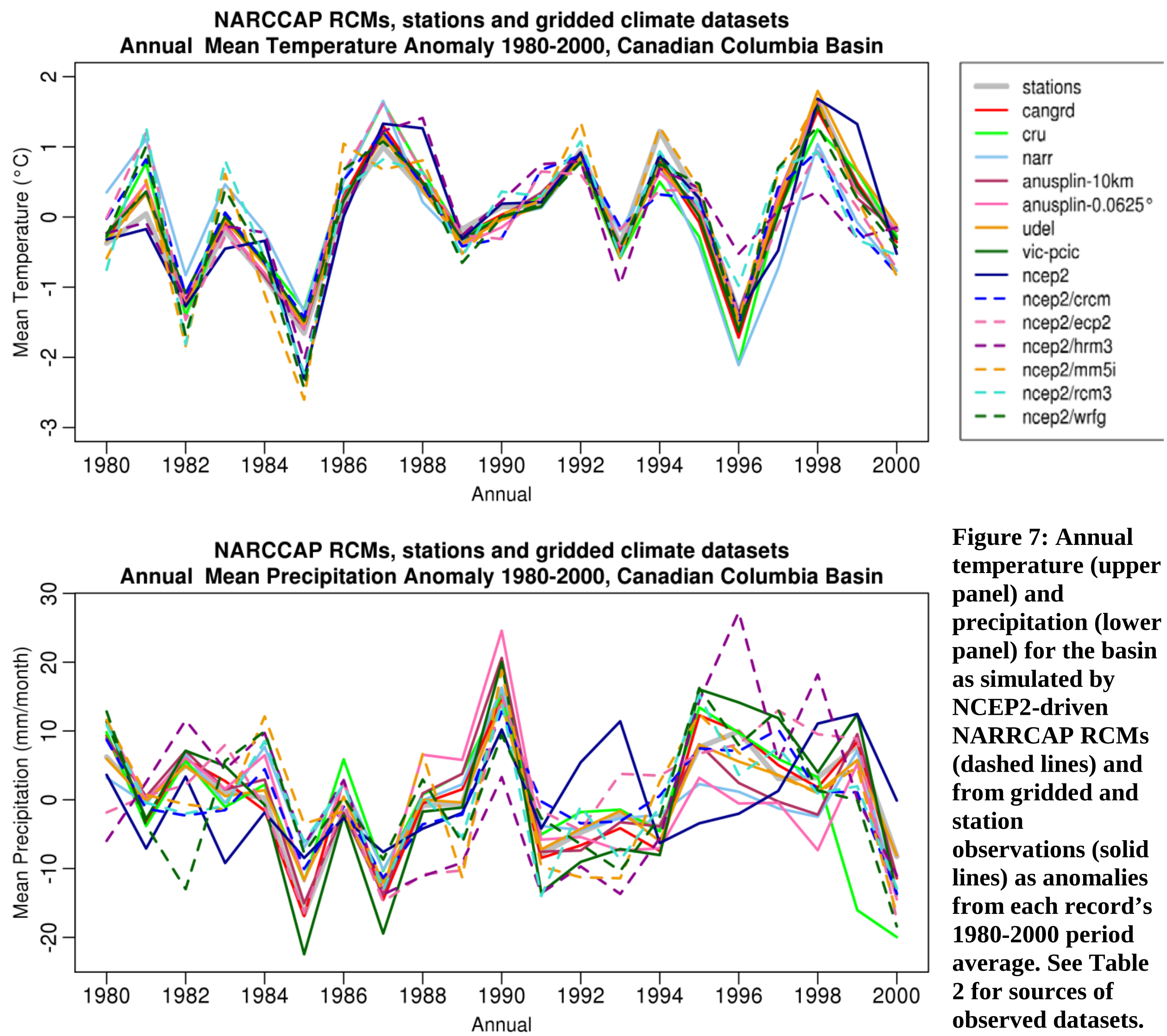

Figure 7: Annual temperature (upper panel) and precipitation (lower panel) for the basin as simulated by NCEP2-driven NARRCAP RCMs (dashed lines) and from gridded and station observations (solid lines) as anomalies from each record's 1980-2000 period average. See Table 2 for sources of observed datasets.

The representation of elevation by each of the RCMs, the observed datasets, stations, and the NCEP2 reanalysis is displayed in Figure 8. Stations clearly misrepresent the reality of the terrain as shown by the 30 arc-second, or roughly 500 m, Digital Elevation Model (DEM) denoted by the black line. Note that DEMs are also uncertain. Stations vastly over-represent the lowest elevations and under-represent all others. The NCEP2 reanalysis, at a resolution similar to GCMs, caps off mountains and fills in valleys, representing the entire area with one elevation.

NARCCAP RCMs do the same to a lesser degree due to their ~50 km resolution. The differences in representation of elevation between RCMs result from the fact that their grids are defined on different map projections. All of the observed gridded datasets relate more closely to observed hypsometry, particularly CANGRID and ANUSPLIN which have elevation corrections. Contrary to what might be expected, there does not seem to be a coherent relationship between differences in RCMs' representation of elevation and historical bias. For example, the model with the warmest bias, HRM3, has the most high elevation locations among all of the RCMs. This suggests that other differences between RCMs such as parameterizations, representations of physics, and land surface schemes (Appendix 2) account for more of the difference in historical climate than direct effects of slightly different representations of topography (Table 3, Figures 6, 7, and 8).

Table 3: Comparison of NCEP2 and NCEP2 driven RCM anomalies from their respective 1980-2000 averages to CANGRID 1980-2000 anomalies from average as well as bias (difference of 1980-2000 average from CANGRID) for annual and seasonal temperature and precipitation for the Columbia Basin.

Annual

RCMs	CRCM	ECP2	HRM3	MM5I	RCM3	WRFG	NCEP2
Temperature							
Corr. Coef	0.9	0.9	0.8	0.9	0.9	0.9	0.9
RMSE (^{o}C)	0.3	0.3	0.5	0.5	0.5	0.4	0.4
Bias (^{o}C)	-3.0	-0.2	2.7	-0.7	-0.5	-0.6	-0.8
Precipitation							
Corr. Coef	0.8	0.7	0.6	0.7	0.8	0.7	0.4
RMSE (mm/month)	5	6	9	7	5	7	8
Bias (mm/month)	-8	10	-6	13	13	6	-36

Winter

RCMs	CRCM	ECP2	HRM3	MM5I	RCM3	WRFG	NCEP2
Temperature							
Corr. Coef	0.9	0.9	0.8	0.9	0.9	0.9	1.0
RMSE (^{o}C)	0.8	0.9	1.2	1.1	1.0	1.4	0.4
Bias (^{o}C)	-3.4	-1.0	3.1	0.3	0.6	-0.8	0.3
Precipitation							
Corr. Coef	0.8	0.8	0.7	0.7	0.7	0.6	0.9
RMSE (mm/month)	11	13	24	19	15	19	10
Bias (mm/month)	-8	8	19	47	33	23	-49

Spring

RCMs	CRCM	ECP2	HRM3	MM5I	RCM3	WRFG	NCEP2
Temperature							
Corr. Coef	1.0	0.9	0.9	0.8	0.8	0.8	0.9
RMSE (^{o}C)	0.4	0.6	0.7	1.1	0.9	0.8	0.5
Bias (^{o}C)	-4.4	-0.9	1.2	-2.1	-1.8	-0.2	-2.7
Precipitation							
Corr. Coef	0.8	0.5	0.4	0.5	0.6	0.6	0.5
RMSE (mm/month)	6	13	11	14	12	12	9
Bias (mm/month)	-14	29	10	16	18	11	-37

Summer

RCMs	CRCM	ECP2	HRM3	MM5I	RCM3	WRFG	NCEP2
Temperature							
Corr. Coef	0.9	0.8	0.6	0.8	0.6	0.8	0.6
RMSE (^{o}C)	0.3	0.4	1.0	0.6	1.0	0.8	1.1
Bias (^{o}C)	-2.1	0.9	3.8	-0.4	-0.3	-0.6	-1.2
Precipitation							
Corr. Coef	0.8	0.7	0.6	0.7	0.7	0.7	0.5
RMSE (mm/month)	9	16	13	10	13	10	20
Bias (mm/month)	2	8	-41	-21	-13	-16	-13

Fall

RCMs	CRCM	ECP2	HRM3	MM5I	RCM3	WRFG	NCEP2
Temperature							
Corr. Coef	0.9	0.9	0.8	0.9	0.9	0.9	0.9
RMSE (^{o}C)	0.6	0.6	1.0	0.8	0.7	1.0	0.6
Bias (^{o}C)	-2.5	0.0	2.5	-0.6	-0.6	-0.9	0.1
Precipitation							
Corr. Coef	0.8	0.8	0.7	0.9	0.8	0.7	0.8
RMSE (mm/month)	12	12	18	12	15	19	13
Bias (mm/month)	-12	-4	-11	12	15	8	-46

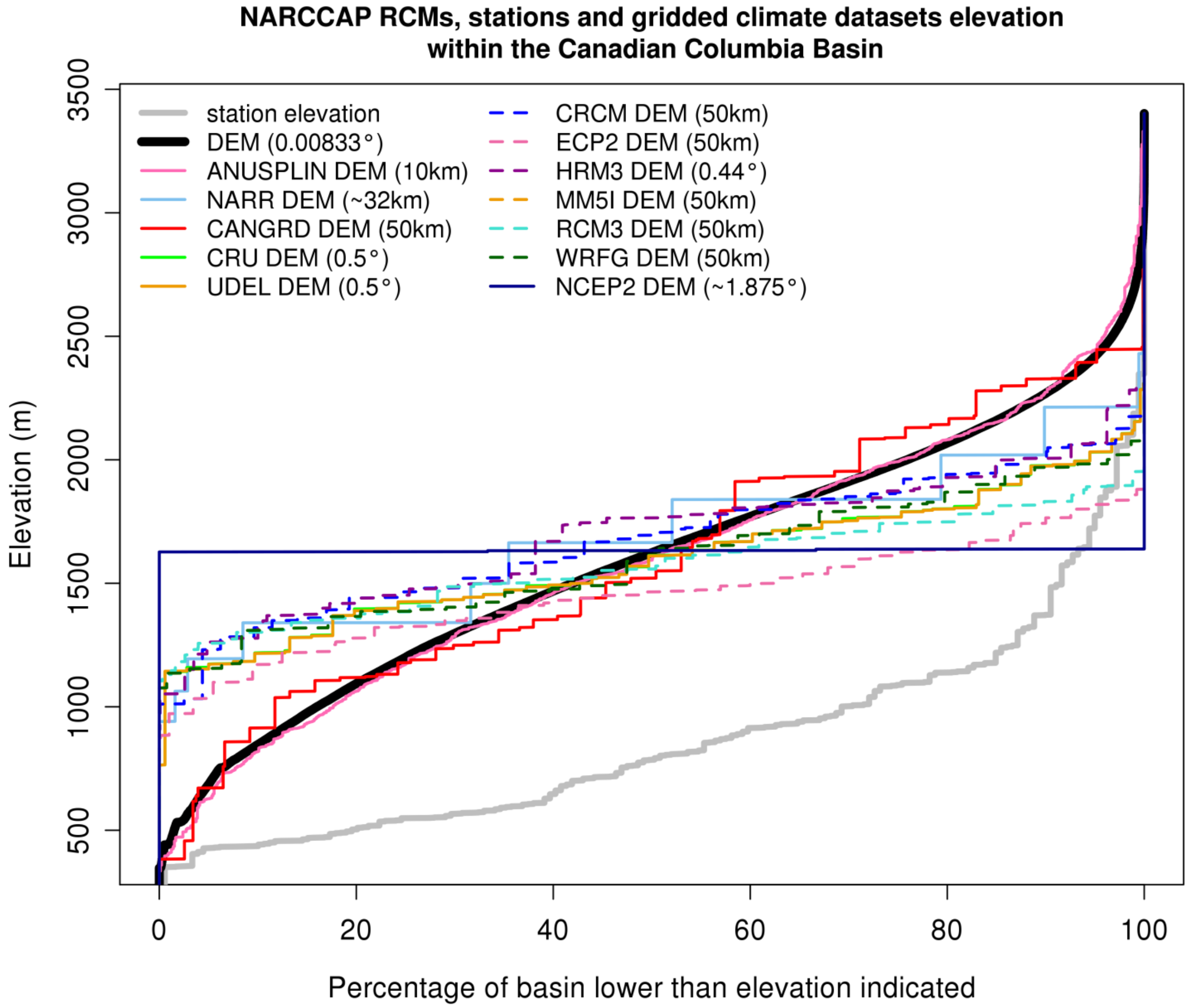

Figure 8: Representation of elevation in each NARCCAP RCM and each of several observational datasets in the Canadian Columbia River Basin. See Table 2 for sources of observed datasets.

3.2. Seasons and sub-regions

While only the basin average is shown in Figures 6 and 7 and in Table 3, results are generally similar for all four sub-regions shown in Figure 1 (Columbia Shuswap, Northern East Kootenay, West Kootenay, and Southern East Kootenay). For example, the distribution of temperature biases throughout sub-regions differs slightly between models (not shown). HRM3 has a warm bias across almost all sub-regions and seasons. While CRCM has a cold bias for most sub-regions and seasons. Of the remainder, most are in agreement with observations or have slight cold biases.

When seasons are considered separately, some differences emerge in bias, but have little effect on anomalies. For example, Figure 9 upper panel shows simulated precipitation for winter. Comparison with Figure 6 lower panel reveals that most RCMs have a wet bias in winter compared to CANGRID. Although they still almost match the spread in observations, the overlap in spread is more on the wet side than for the annual average. When anomalies from the 1980-2000 average are computed (compare Figure 9 lower panel to Figure 7 lower panel), results are fairly similar for winter and for the annual average.

We have seen that the differences between RCM simulations and gridded observations are relatively constant in time throughout the baseline period in Figures 6, 7, and 9, and Table 3, and this holds for all of the sub-regions and seasons as well (not shown). This means that the simulated within-region differences can be illustrated by maps of RCM simulated baselines. In Figures 10 and 11 these maps are shown compared to NCEP2, the elevation-corrected CANGRID dataset we use as a standard for comparison here, and the UDEL dataset which is used as a standard for comparison within NARCCAP (unlike CANGRID which is Canada only, UDEL covers all of North America). Each RCM captures the cold temperatures associated with the highest elevation mountain ranges of the East Kootenays, and the larger precipitation in the Columbia Shuswap region. The RCM simulated historical climatologies are smoother than observations but more representative of within-region differences than NCEP2.

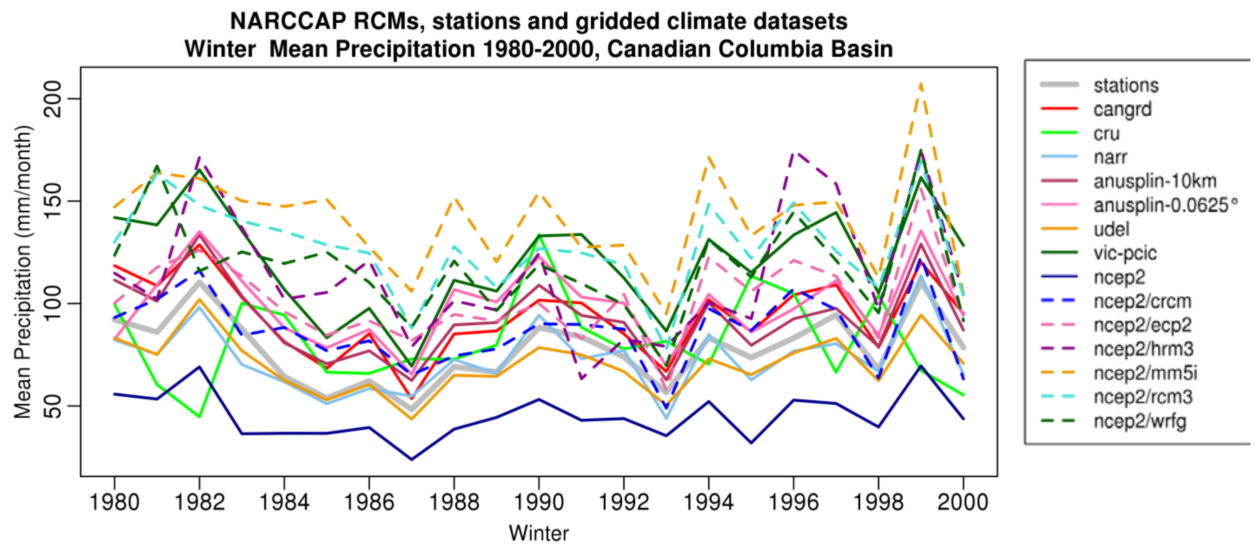

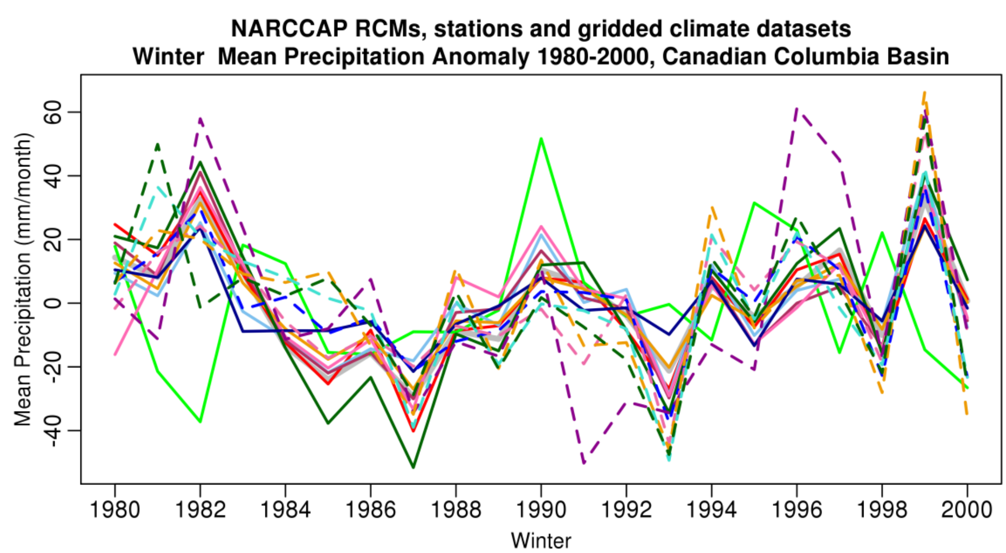

Figure 9: Winter mean precipitation (upper panel) and anomalies from each record's 1980-2000 period average (lower panel) for the basin as simulated by NCEP2-driven NARRCAP RCMs (dashed lines) and from gridded and station observations (solid lines). See Table 2 for sources of observed datasets.

3.3. Value-added

So far we have investigated the ability of RCMs to simulate historical climate. Despite some biases, RCMs are able to capture the year-to-year variations in temperature and precipitation across the basin and each of the sub-regions on both an annually and seasonally averaged basis. The RCMs have less bias than NCEP2 driving data in almost all cases, and are better correlated with CANGRID observations. Thus, they provide improvements in simulating the climate of the basin compared to their coarse resolution driving data. This gives some confidence that, despite the potential for additional uncertainty to arise from the use of RCMs as another tool in the modeling chain, projected future RCM anomalies will differ from those of their driving GCMs and that those differences will represent "value-added" improvements.

Finally, we will investigate the difference between RCMs and their driving GCMs over the basin. We compare the GCM-driven climatology to RCM simulations during the 1971-2000 baseline from which 2050s anomalies will subsequently be calculated. When compared to their driving GCMs over the baseline rather than to NCEP2, almost all RCMs simulate colder temperatures and more precipitation in all seasons, as shown in Figure 12. This result is consistent with RCMs better representing high elevation locations than GCMs.

RCM future projected anomalies (difference of 2050s projection from the corresponding simulated 1971-2000 baseline) compare to projected anomalies from their driving GCMs in a more complicated way. Generally, RCMs project less warming as shown in the left panel of Figure 13. For the two GCMs that drive three RCMs each, it is the case that the RCM with the coldest simulated past has the largest projected anomalies and vice versa (although these cases are too few to indicate a general relationship between historical bias and future projections). In addition, the spread in projected future anomalies is smaller than the spread in simulated baseline climatology, providing some confidence that historical bias does not unduly influence projected future change. These results are fairly similar across the other seasons for temperature (not shown). The effect of RCMs on precipitation anomalies does depend on season and the same driving GCM can produce quite different precipitation anomalies in different RCMs (Figure 14). For example, the CCSM GCM was used to drive three RCMs. In spring and summer some of these RCMs project more precipitation than the CCSM and some less, with a spread of about 13% in both seasons. Too few simulations are available to determine whether or not there is a relationship between differences in RCM and driving GCM anomalies.

In summary, the RCM simulated historical temperature and precipitation compares more closely to observations in almost all cases than its coarse resolution driving NCEP2 according to basic measures of historical skill (bias, correlation, RMSE). Furthermore, this is the case both on a regionally averaged basis and throughout the region. Based on this evidence, RCM simulations are expected to provide improvements to projected future change in the region compared to raw GCM projections.

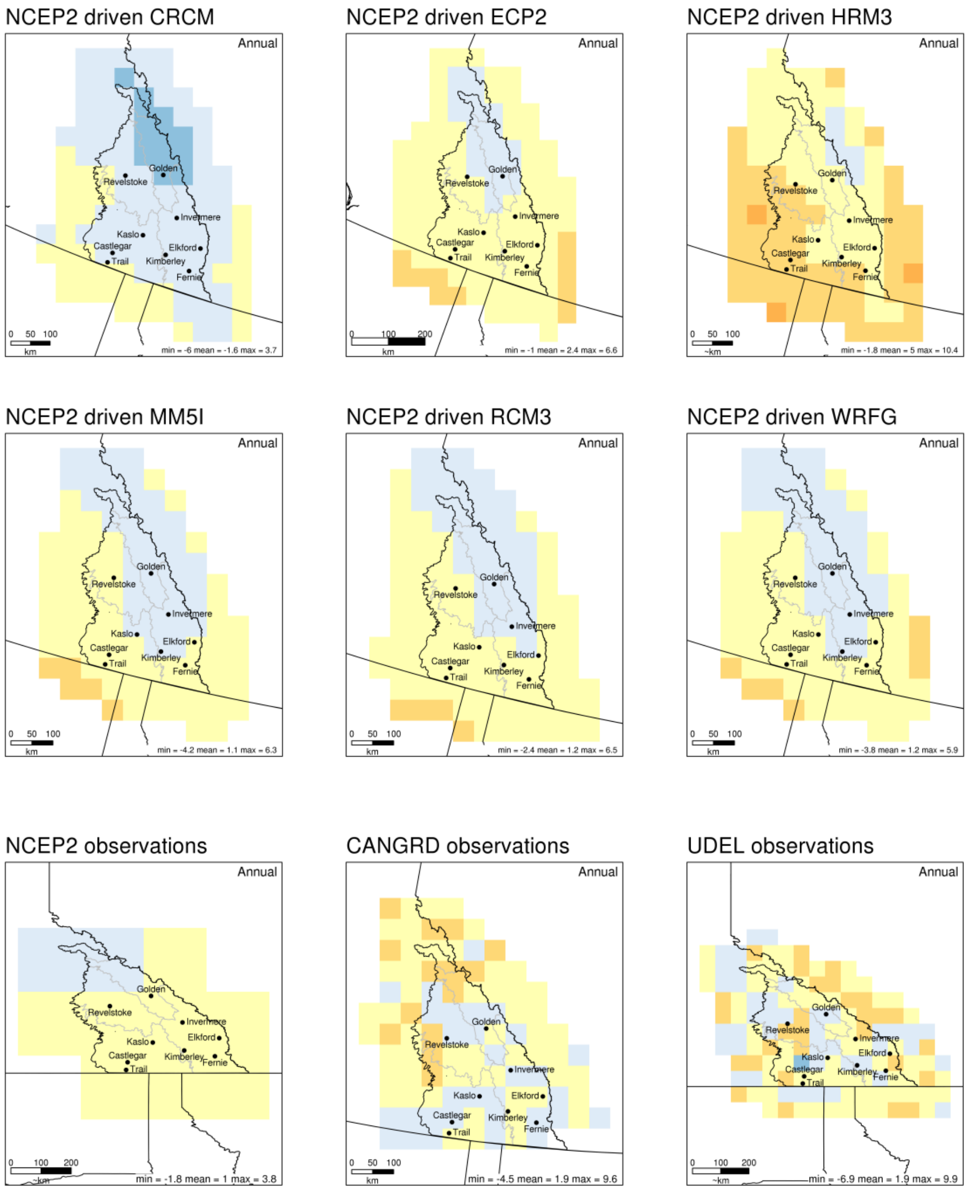

Figure 10: Historical 1980-1999 mean annual temperature simulated by each NCEP2 driven NARCCAP RCM compared to NCEP2 reanalysis of observations and CANGRD and UDEL gridded observations.

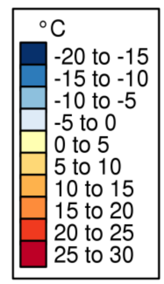

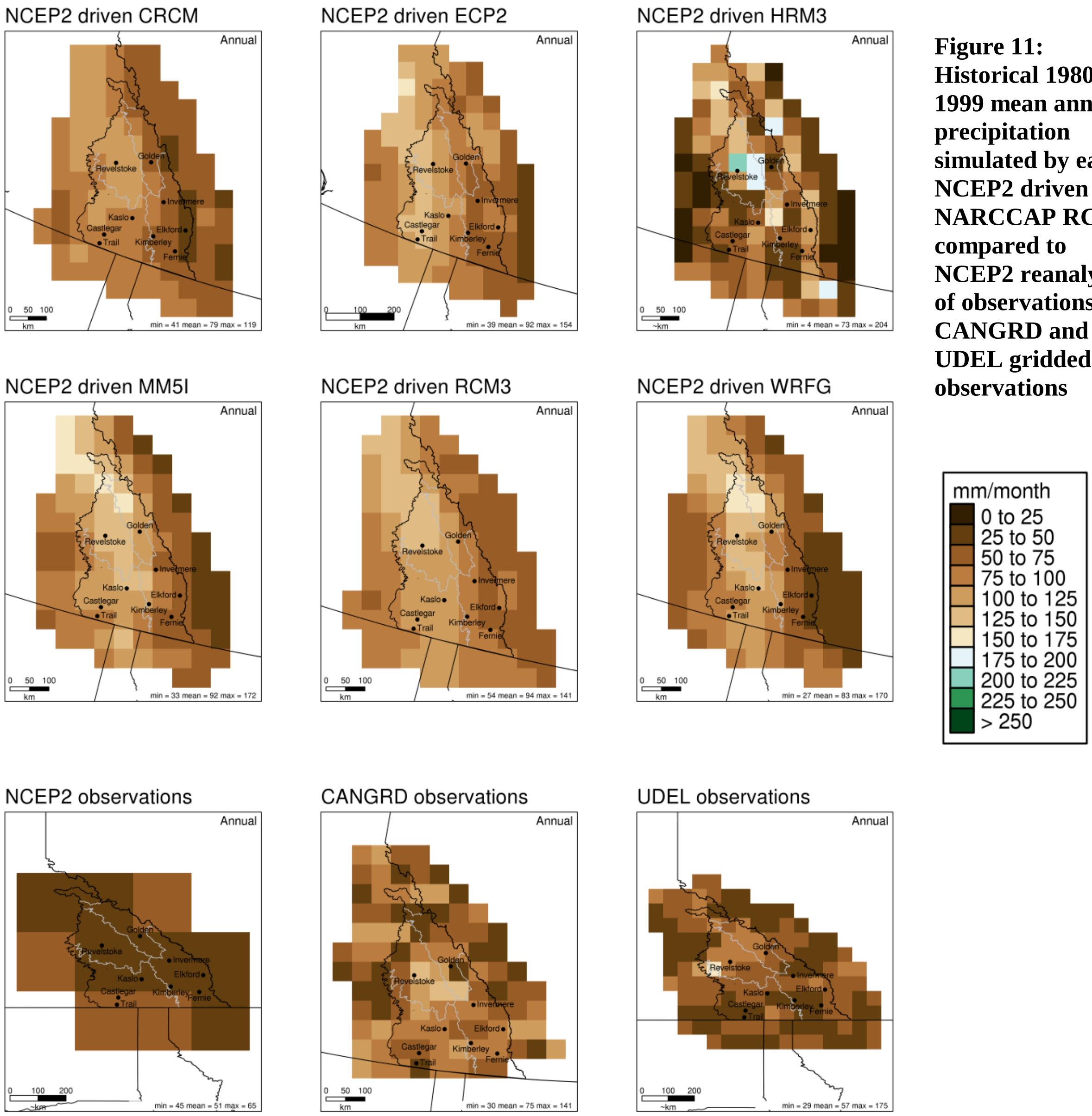

Figure 11: Historical 1980-1999 mean annual precipitation simulated by each NCEP2 driven NARCCAP RCM compared to NCEP2 reanalysis of observations and CANGRD and UDEL gridded observations

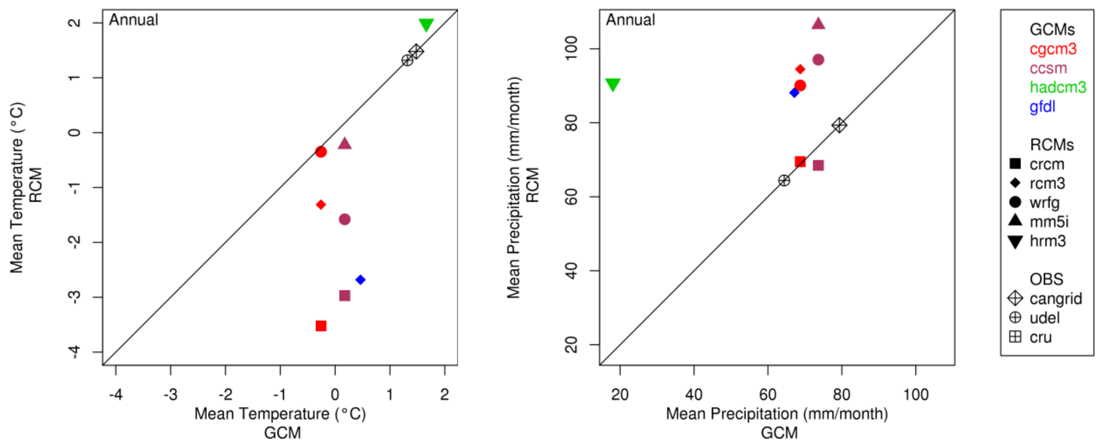

Figure 12: Simulated 1971-2000 annual temperature (left column) and precipitation (right column) according to each NARCCAP RCM run, its driving GCM, and three gridded observational datasets. Colours denote GCMs and symbols denote RCMs.

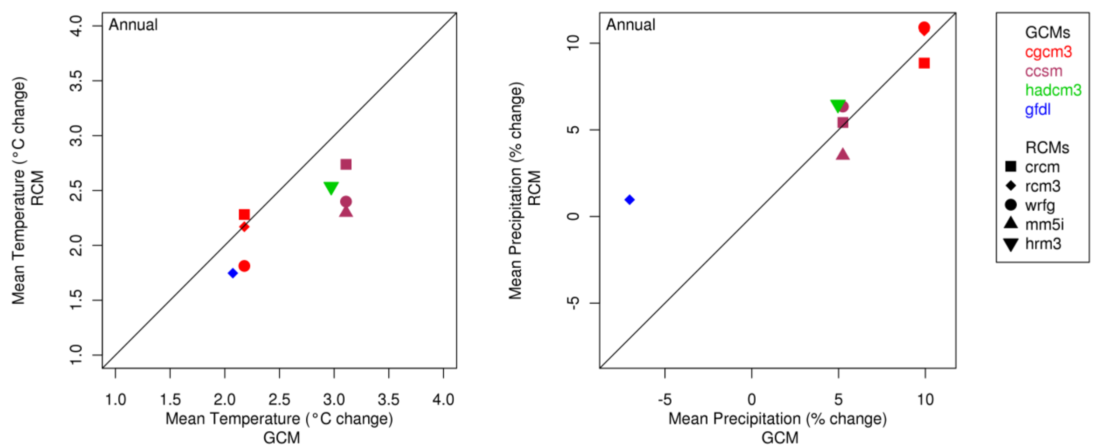

Figure 13: Projected 2050s future annual temperature (left column) and precipitation (right column) change according to each NARCCAP RCM run and its driving GCM. Colours denote GCMs and symbols denote RCMs.

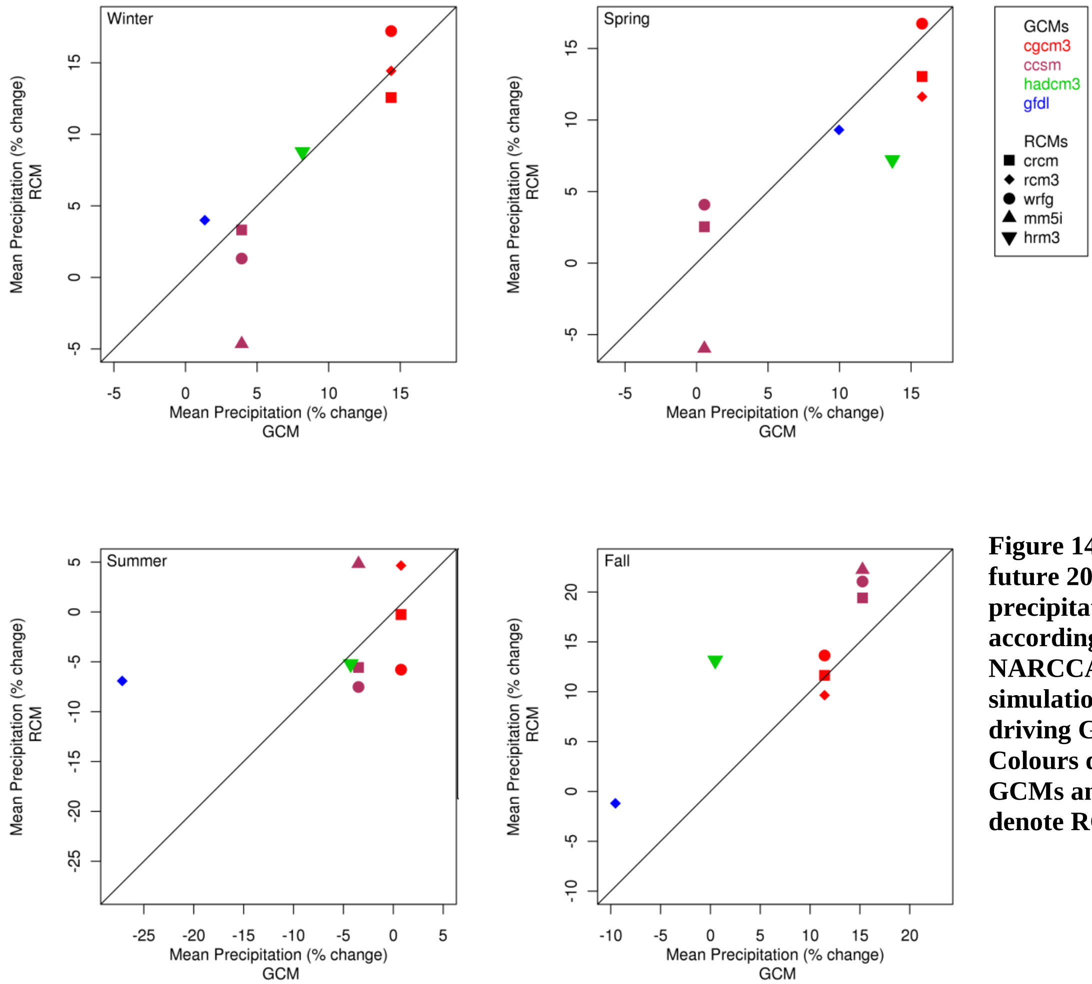

Figure 14: Projected future 2050s seasonal precipitation change according to each NARCCAP RCM simulation and its driving GCM. Colours denote GCMs and symbols denote RCMs.

4. Future projections – results and discussion

Now that we have evaluated the ability of RCMs to simulate the past in the region and provided evidence that they add some value compared to coarse scale information, we will consider RCM projected changes including indices of extremes. Table 4 shows the RCMs and driving GCMs that make up the members of the ensemble of future projections. Of the six RCMs assessed in the previous section, all but ECP2 have future projections available. There are two runs from CRCM, RCM3, and WRFG and one run from MM5I and HRM3. The driving GCMs are CGCM3 and CCSM with three RCM runs each plus one driven by each of HadCM3 and GFDL.

Results are described and summarized for most indices, but only some are shown visually. The choice of which results to present in map form was based on relevance and applicability of results to other indices. In cases where there is less variation in results only lowest, medium, and highest change are shown (e.g., Figure 15). In other cases where results differ more throughout the basin for different runs, all eight are shown (e.g., Figure 16 and 17).

Table 4: RCM future projection ensemble members and driving GCMs. An X indicates an ensemble member driven by the GCM listed in the row for the RCM listed in the column. See Table 11 in Appendix 2 for additional information on each RCM.

		RCM run						
		CRCM	ECP2	HRM3	MM5I	RCM3	WRFG	*Total*
Driving GCM	CGCM3	X				X	X	3
	CCSM	X			X		X	3
	GFDL					X		1
	HadCM3			X				1
	Total	2	0	1	1	2	2	8

Basin-average change in mean and variability

The ensemble of eight projections shows a range of basin-average warming of 1.8°C to 2.7°C by the 2050s compared to 1971-2000. Three runs are shown in Figure 15, representing the least, middle, and most basin-averaged warming. Projected annual mean temperature change is quite coherent across the basin in all runs (Table 6), a result that generally holds for all seasons as well. The standard deviation of inter-annual temperature during the baseline according to CANGRID is roughly 1.0°C at most locations and 0.8°C (not shown) for the basin-average, considerably smaller than the projected range of warming by the 2050s.

The basin-averaged projected annual precipitation change by the 2050s is +1% to + 9% of the 1971-2000 average, as shown in Figure 16. The standard deviation of inter-annual precipitation according to CANGRID gridded observations during the baseline is roughly 30% of the 1971-2000 average at most locations (not shown), so the projected changes to precipitation are not as large in comparison to historical variability as for temperature. The pattern of change differs throughout the region for different runs with larger precipitation increases projected in most cases for the Columbia Shuswap and Northern East Kootenay regions (see Figure 1 for sub-region names and boundaries), particularly by the CGCM3 driven runs. The projected change in precipitation varies considerably between seasons and runs (Figure 17).

Projected changes in the standard deviation of temperature (not shown) are very close to zero and quite uniform across the basin. This indicates that year-to-year variability in future is similar to that of the past in these simulations, although the ensemble is not large enough to make a definitive statement about whether this is a feature of the particular ensemble we have chosen or a robust projection for the future. However, it suggests that changes in extremes in our ensemble are mostly the result of changes in average temperature rather than changes to variability in the future projections. Projected changes in standard deviation of precipitation (not shown) vary considerably by time of year and run.

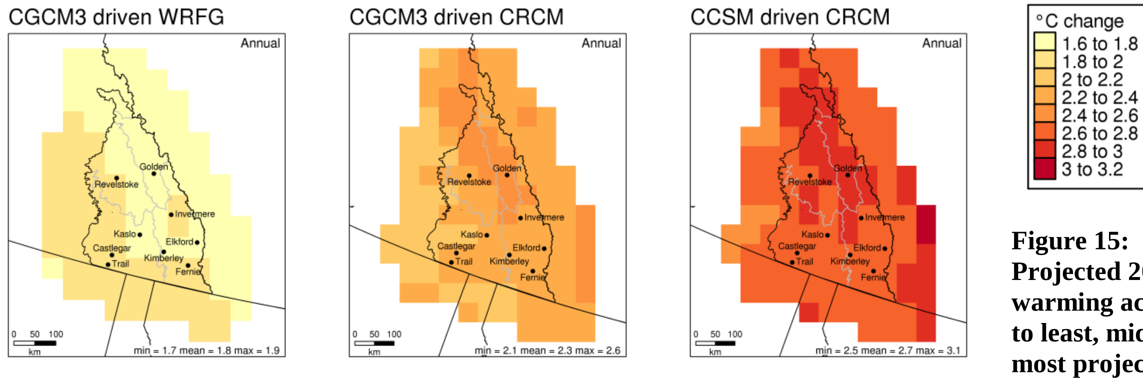

Figure 15: Projected 2050s warming according to least, mid, and most projected basin average change.

Ranges of change

Note that ranges in results are provided in different ways in this report. Throughout section 4, the main range of projected change reported is that of basin-averaged change from all 8 runs. In Appendix 1, tables are provided that include the range of projections among individual grid boxes as well. Tables 6 through 9 provide annual quantities while Table 5 also includes the range of results from different months of the year as well. The ranges in Appendix 1 can be compared to the basin-averaged changes reported throughout section 4 to determine how representative the basin-average is for a given variable. For example, the basin-average annual temperature change (1.8°C to 2.7°C) happens to be identical to the 10th to 90th percentiles[v] of annual temperature change and the full range from all grid boxes is not much wider (1.7°C to 3.1°C; Table 6), consistent with the spatially coherent warming depicted in Figure 15. In addition, the projected change depends relatively little on the month of the year for temperature: the 10th to 90th percentiles of all monthly projections for all runs and grid boxes is 1.3°C to 3.4°C (Table 5), only marginally larger than the range for the annual average. Some locations do show considerable differences from this majority during some times of the year, however (from 0.4°C to 5.1°C; Table 5).

The 10th to 90th percentile range of projected annual precipitation change at individual grid boxes is +1% to +12% (Table 6).This is a wider range than the range in basin-average change, indicating that projected annual precipitation changes vary spatially considerably throughout the region (Figure 16). Furthermore, the 10th to 90th percentile range when including projections from all months of the year is much wider (-12% to +26%; Table 5), consistent with projected precipitation changes that vary considerably by season (Figure 17).

[v] Percentiles are based on the individual grid box projected changes at the ~110 grid boxes per model shown in the maps. These individual changes include changes at individual grid boxes nearby the Basin.

It must be noted that none of these ranges, even the basin-averages, are directly comparable to regionally averaged changes from large ensembles of GCMs and multiple emissions scenarios. There are three important differences between the RCM projections from NARCCAP (Figures 15 to 23) and ensembles of GCM projections commonly used, such as the PCIC30 ensemble (Figures 3, 4, and 5). These differences, described below, are important to consider when comparing results in this section to ensembles of GCM results.

The main difference is the small number of GCMs (4) used to drive the members of the NARCCAP ensemble (Table 4) as opposed to 15 GCMs in the PCIC30. In addition, NARCCAP runs are driven by the SRES A2 emissions scenario only. Projected climate change in British Columbia by the 2050s is slightly larger for the A2 (1.2°C to 2.5°C) than B1 (1.2°C to 2.1°C) runs in the PCIC30 ensemble (Rodenhuis et al. 2009). A comprehensive understanding of uncertainty and most likely range of projected change cannot be derived from these results alone. Rather, mean temperature and total precipitation are included to assist with interpretation.

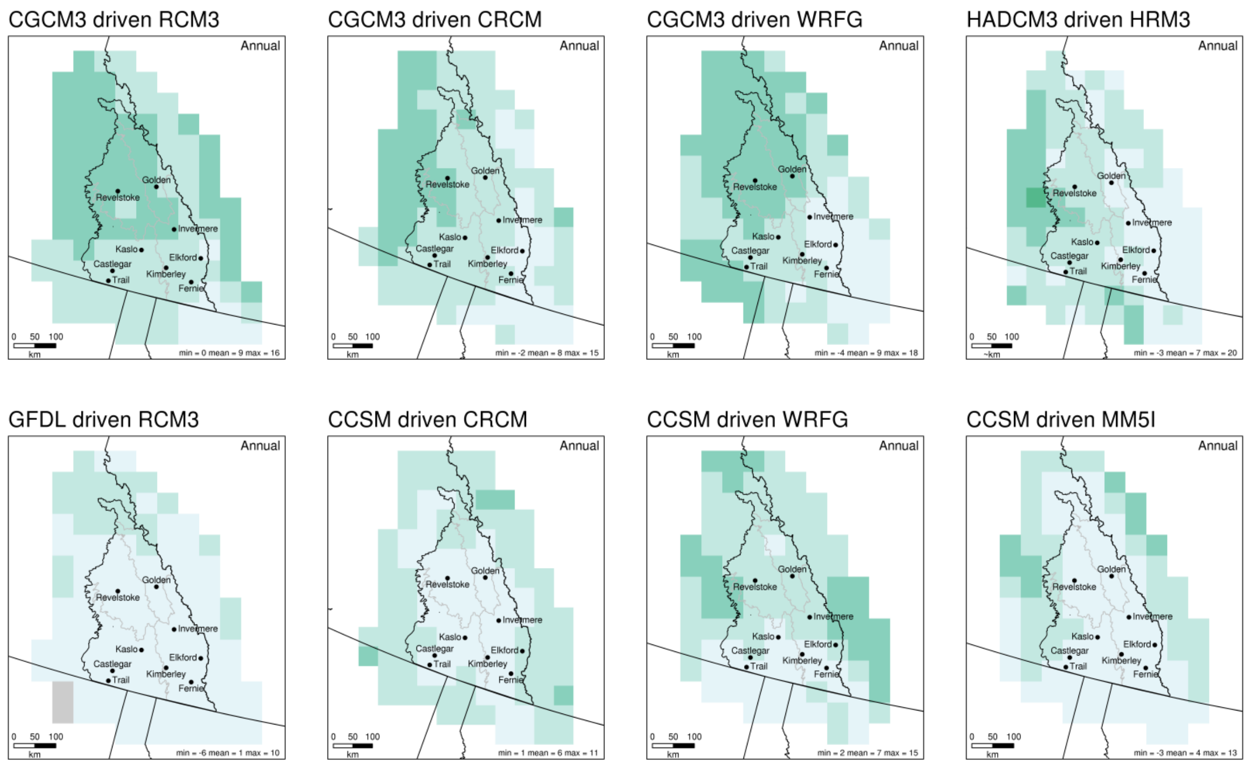

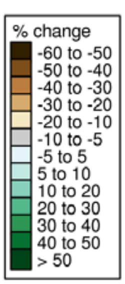

Figure 16: Projected 2050s change in annual precipitation according to all eight available RCM runs.

Finally, all 2050s projected changes are from a 1971-2000 baseline. This differs from the 1961-1990 baseline used in most previous analysis in the region. Gridded CANGRID observations for these two periods indicate that 1971-2000 was warmer by 0.1°C for day time highs, 0.2°C for night time lows, with less precipitation in winter (-2%) and more in spring (+5%), summer (+4%), and fall (+2%) compared with 1961-1990.

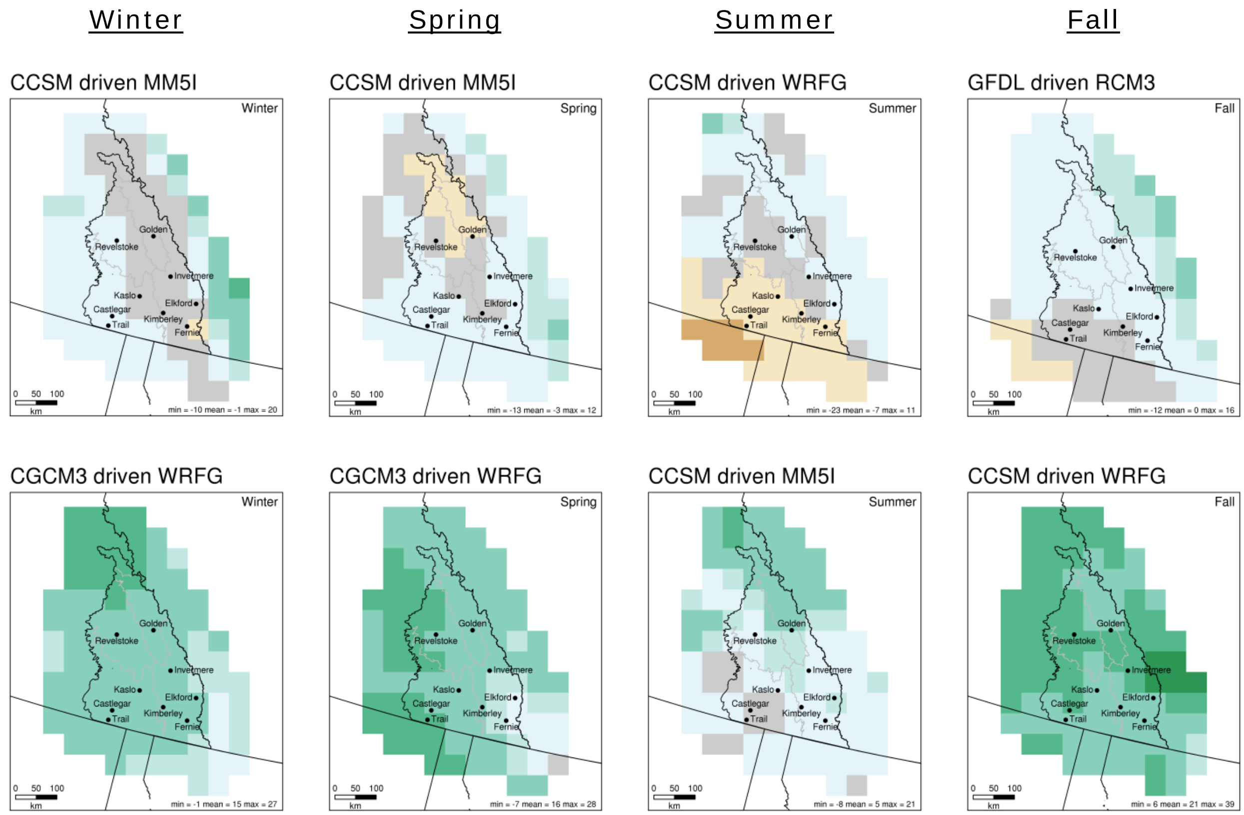

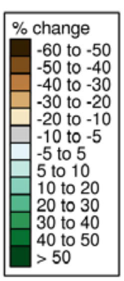

Figure 17: Projected 2050s largest decrease (top row) and largest increase (bottom row) in basin average seasonal precipitation.

4.1. Percentiles

Percentiles are a general indicator of changes in extremes (see description Section 2). For temperature, we analyze the number of days that are warmer than the 10th and 90th percentiles of daytime high (maximum) temperatures from 1971-2000 for each day of the year based on a 5-day window surrounding each day of the year, and conversely cooler than these percentiles for nighttime low (minimum) temperatures. For precipitation, we consider the amount of precipitation that falls during very wet days when precipitation is above the 95th and 99th percentiles of precipitation amounts from the baseline.

- Cool nights - TN10p: occurrence of minimum temperature frequency < 10p
- Warm days - TX90p: occurrence of maximum temperature frequency > 90p
- Cool days - TX10p: occurrence of maximum temperature frequency < 10p
- Warm nights - TN90p: occurrence of minimum temperature frequency > 90p
- Very wet day precipitation - R95pTOT: annual total precipitation when > 95p
- Extremely wet day precipitation - R99pTOT: annual total precipitation when > 99p

Projected changes in occurrence of temperature percentiles are quite uniform throughout the basin. The following ranges of change are all based on basin averages but the ranges for individual grid boxes are only slightly wider in most cases (see Appendix 1).

The runs projecting most and least change in warm days (TX90p) in summer and cool nights (TN10p) in winter are shown in Figures 18 and 19. Regionally averaged warm days in summer are projected to become 1.3 to 3.4 times more frequent than in the past and up to 4.2 times as often as some locations. Cool nights in winter, however, are projected to occur less often than in the past: 0.7 to 0.4 times as often for the region.

Warm nights (TN90p) in summer, important for health impacts, are projected to increase by a slightly larger factor than warm days: 2.0 to 4.0 times as often as in the past for the region as a whole. Cool days (TX10p) in winter are projected to occur 0.7 to 0.6 times as often as in the past for the regional average.

Almost all runs project an increase (2% to 8%) in the *amount* of precipitation that falls during very wet days (R95pTOT; Table 7). Most runs indicate an increase (0% to 4%) in the precipitation amount of extremely wet day precipitation (R99pTOT; Table 7) as well, but the agreement is less consistent throughout the basin and across the runs than for R95pTOT. Both are shown in Figure 20 for all runs.

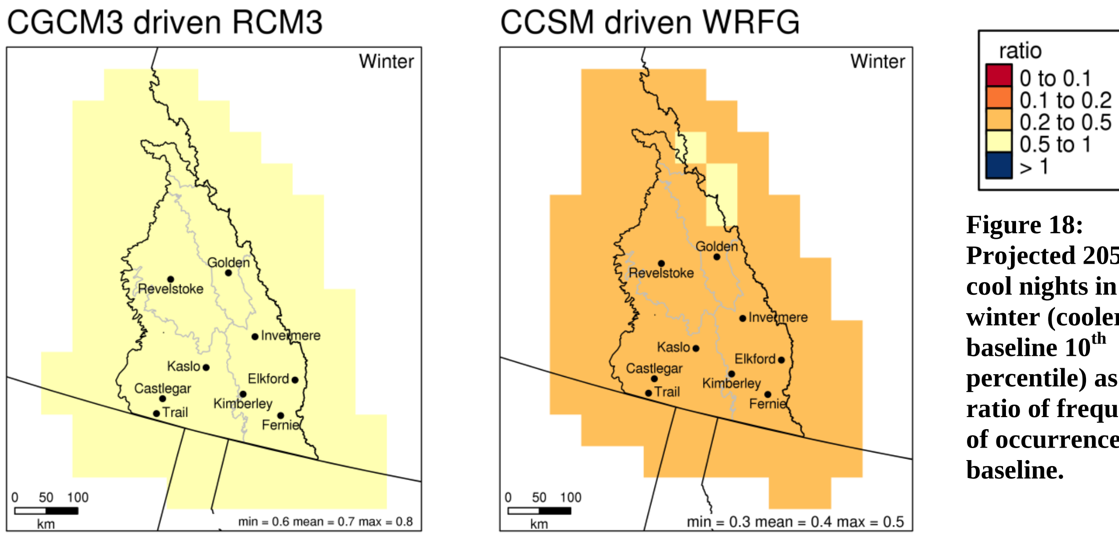

Figure 18: Projected 2050s cool nights in winter (cooler than baseline 10th percentile) as a ratio of frequency of occurrence in baseline.

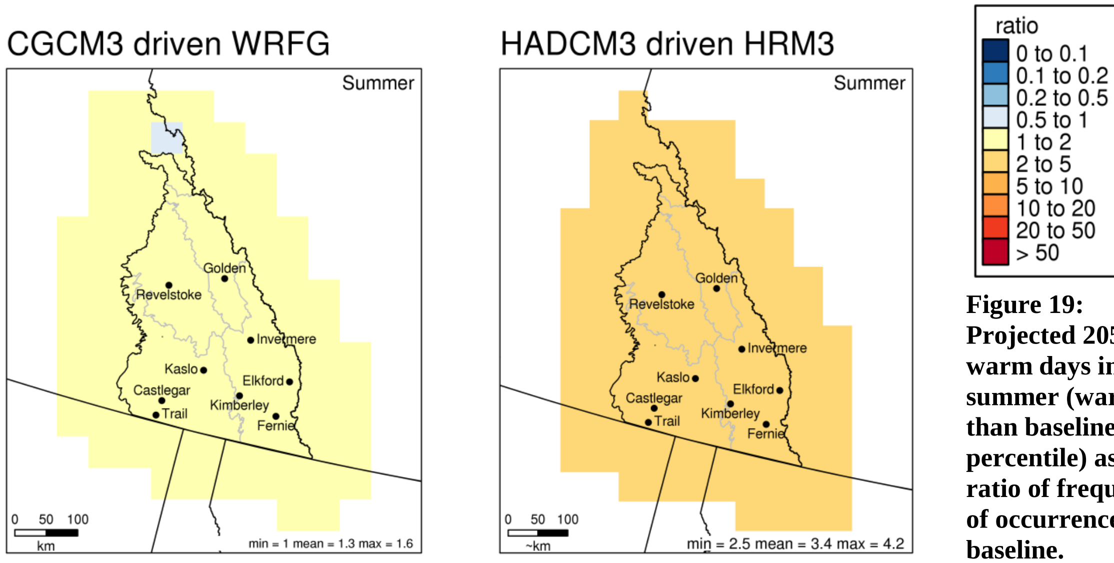

Figure 19: Projected 2050s warm days in summer (warmer than baseline 90th percentile) as a ratio of frequency of occurrence in baseline.

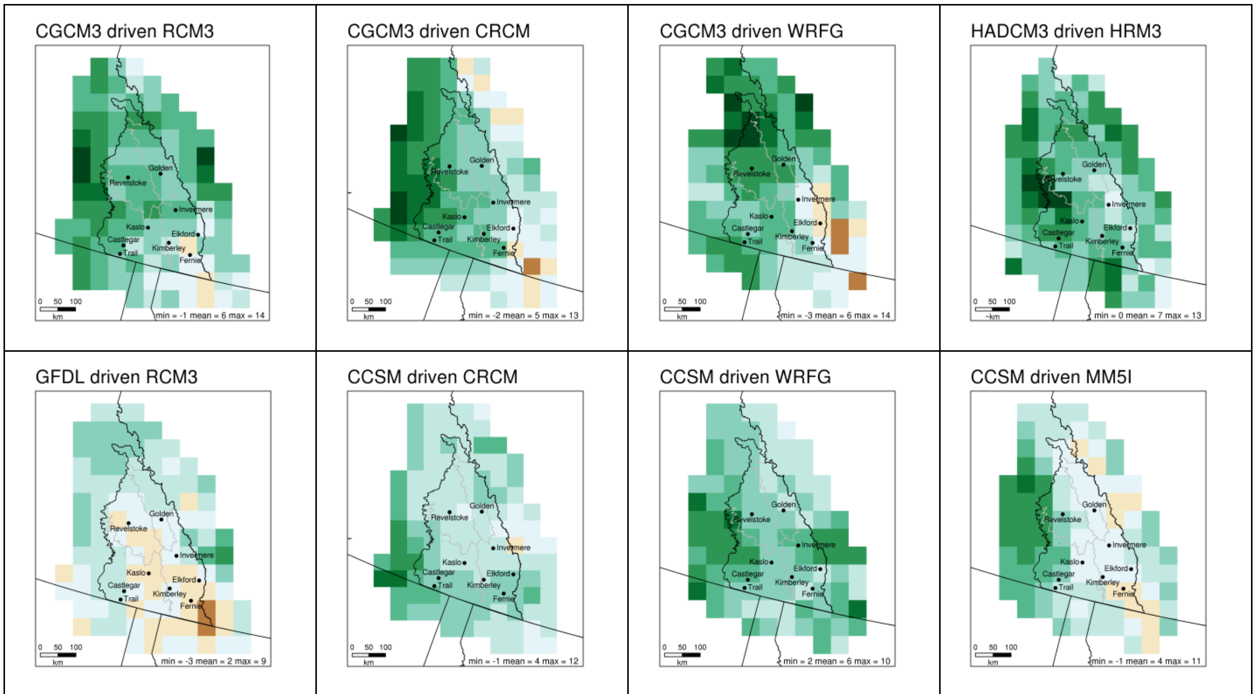

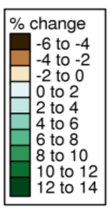

Figure 20: Projected change in 2050s annual total precipitation on very wet days (R95pTOT; above) and extremely wet days (R99pTOT; below) as a percent of 1971-2000 baseline total annual precipitation.

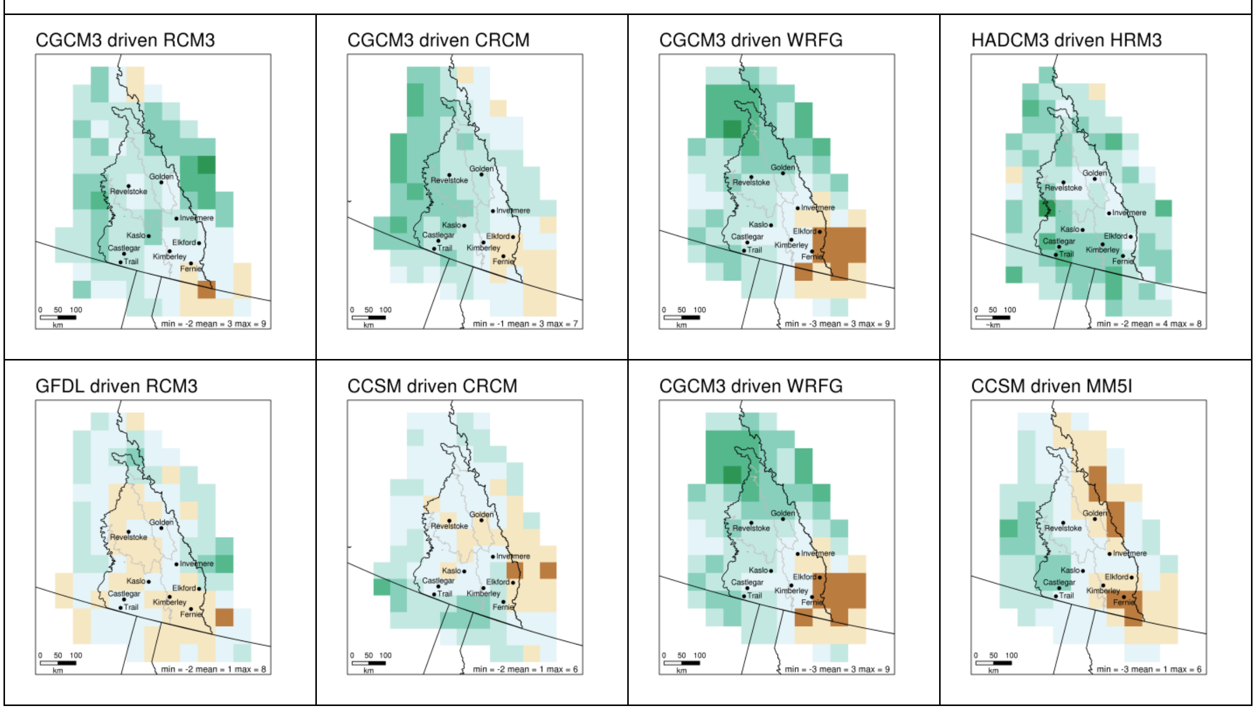

4.2. Return periods

The results in this section are based on the best estimates of the three GEV parameters (see section 2.2 for a description of how return periods are computed). The spatial range in results at individual grid boxes is given for temperature and precipitation in Table 8. Additional uncertainty arising from the confidence intervals of estimates of the GEV parameters is given in Tables 9 and 10 (fits are made independently at each grid box).

Warm temperature events that in the past had 5-year return periods are projected to occur about 2 to 4 times more often in future, on average over the basin (Figure 21). For the 10-year and 25-year return periods, the ratios are about 2 to 6 and 2 to 11 times more often, respectively (Figure 22). These results describe a new climate by the 2050s in which return periods can no longer be considered static but express instead the likelihood of occurrence of an event of a particular size at a given time. In other words, what was in the past a 25-year event had a 4% chance of occurring per year in the baseline. For the run with the largest change where this event is projected to increase in frequency by a factor of 11, that same event will have a 44% chance of occurring in future (on average over the 30 year period). These results are consistent with the GCM results shown in Figure 2. Many of the runs project the largest changes in the two southern sub-regions, with some exceptions (Figure 22). Projected changes in temperature return periods are quite coherent spatially, with similar results for the 10^{th} to 90^{th} percentiles of all changes (Table 8) as for the basin-average ranges (displayed on Figures 21 and 22).

The median projection for cold temperature events is a ratio of 0.3 times as often as in the past for 5-, 10, and 25- year return periods (Table 8). The 10^{th} to 90^{th} percentile range is almost uniform across all three return periods as well, from 0.1 or less to 0.6, which indicates that cold events are projected to occur from two-thirds as often as in the past to one tenth or less. The range of uncertainty in upper and lower bounds is fairly wide for the cold events – including projections of cold extremes disappearing entirely (Table 9) or becoming more frequent (Table 10).

On average over the basin, the occurrence of 3-hourly precipitation events corresponding to the historical 5- and 10-year return periods are projected to double in frequency, and to increase by a factor of 2 to 3 for the 25-year return period. Projected changes at individual grid boxes demonstrate considerable variation from these ratios (Table 8). Several runs project the largest increases in the Columbia Shuswap sub-region and smallest increases generally in the Southern East Kootenay. The ratio of increase in the return periods was slightly smaller for 24-hour events than 3-hourly events (Tables 8 and 9).

Snow depth projections were available only from CGCM3 driven CRCM and CCSM driven WRFG. These two runs generally projected a decrease in the frequency of 5, 10, and 25-year return period events throughout the basin including the complete disappearance of events in some cases. However, some locations were projected to experience increases as well, by as much as a factor of 4 for the 25-year return period.

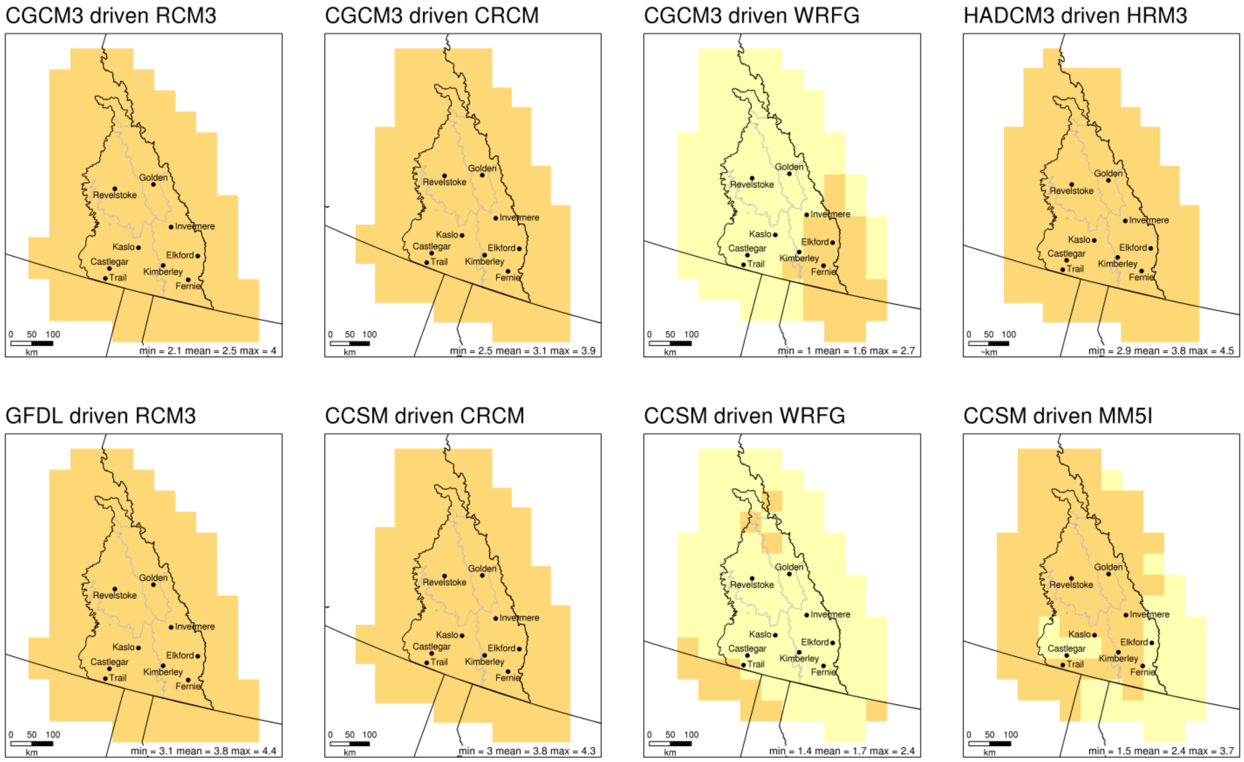

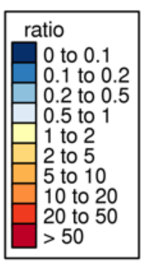

Figure 21: Frequency of baseline 5-year return period temperature (daily; right side) as ratio of occurrence in 1971-2000 baseline.

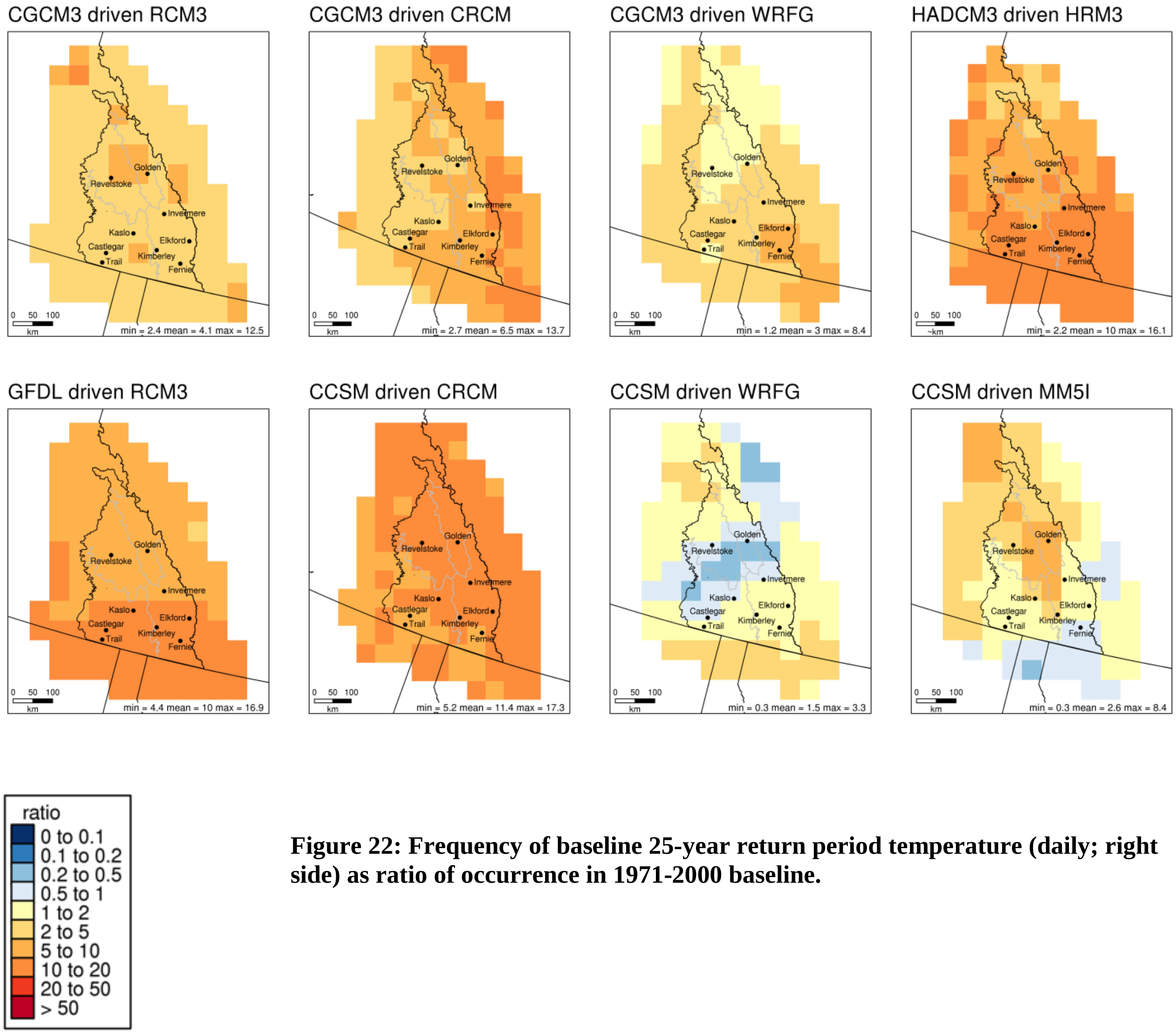

Figure 22: Frequency of baseline 25-year return period temperature (daily; right side) as ratio of occurrence in 1971-2000 baseline.

4.3. Simple temperature and precipitation indices:

- Daily temperature range - DTR: diurnal temperature range
- Hottest day - TXx: monthly maximum value of daily maximum temperature
- Hottest night - TNx: monthly maximum value of daily minimum temperature
- Coldest day - TXn: monthly minimum value of daily maximum temperature
- Coldest night - TNn: monthly minimum value of daily minimum temperature
- Heaviest precipitation day - RX1day: monthly maximum 1-day precipitation
- Heaviest 5-day precipitation - RX5day: monthly maximum consecutive 5-day precipitation

Most runs project a reduction in the annual average diurnal temperature range (DTR) throughout the basin of 0°C to 1°C (Table 6). This would represent a continuation of the historical trend towards larger increases in night time low temperature than in daytime high temperature in the region (Murdock et al. 2007). In most cases, this effect is concentrated in the winter season, though it is also present in shoulder seasons. The largest disagreement between runs is for summer diurnal temperature range where nearly equal numbers of runs project decreases (of up to 0.5°C) as increases (of up to 0.5°C). Note, that the six GCMs that include both minimum and maximum temperature available on the PCIC Regional Analysis Tool[vi] project very little change in DTR, but the projected decrease in DTR for this region according to the RCMs agrees with the multi-model average from a large number of GCMs (see Figure 10.11 in Meehl et al., 2007). It is interesting to note that in most areas of the globe changes in DTR that occurred in the mid 20th century ended in recent decades, and minimum and maximum temperatures have warmed at similar rates (Meehl et al., 2007).

The basin-average hottest day of the month (TXx) is projected to warm by a range of 0.3°C to 4.7°C depending on the run and month. Projections at individual grid boxes vary widely from these basin-average values – from slight decreases to increases of 10.5°C to 11.7°C for April, May, and June in CCSM driven MM5I, as shown in Figure 23. Most changes are between 0.7°C to 3.6°C (10th to 90th percentile of changes from all grid boxes, runs, and months; see Table 5). Some runs project the largest increases in the Northeastern Kootenay sub-region while others project the largest increases in the two southern sub-regions. The instances with unusual changes in TXx (largest warming and cooling in some locations) appear to be in locations and times of year when historical simulated TXx was often near freezing. Further work would be required to determine the mechanism responsible for these results.

The basin-averaged coldest night of the month (TNn) is projected to warm by near zero change up to 7.8°C, depending on the run and month (Table 5). The largest warming in TNn at any location is 10.6°C by CCSM driven WRFG in February. There is little agreement between models as to which sub-regions will experience the most warming in TNn.

The basin-average coldest day (TXn) is projected to warm by 1.3°C to 4.2°C in January and 0.9°C to 4.1°C in July. The basin-average warmest night (TNx) is projected to warm by 0.3°C to 3.7°C in January and 1.4°C to 3.4°C in July.

The basin-average heaviest monthly precipitation day (RX1day) is projected to change by anywhere from -3 mm to +5 mm with decreases generally in summer months and increases from September through November. For the heaviest monthly consecutive 5-day precipitation (RX5day) the range of projected change is -6 mm to +14 mm with the largest decreases in February and largest increases in November.

[vi] http://pacificclimate.org/tools-and-data/regional-analysis-tool date accessed 12 January 2012

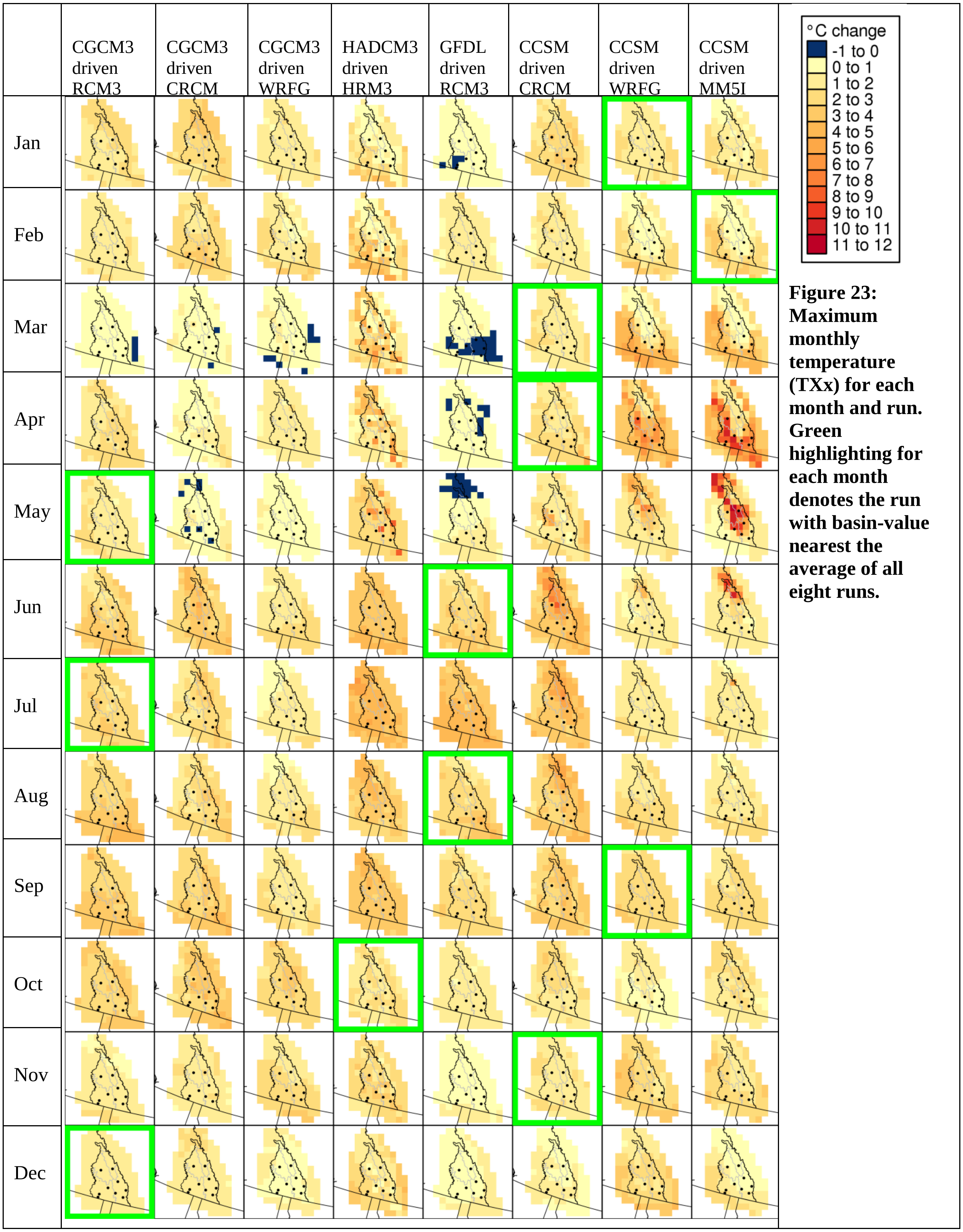

Figure 23: Maximum monthly temperature (TXx) for each month and run. Green highlighting for each month denotes the run with basin-value nearest the average of all eight runs.

4.4. Complex indices

Analysis of CLIMDEX indices as simulated by several statistical downscaling methods indicates less skill for complex than for simpler indices (Bürger et al. 2012). Whether RCMs are better able to simulate these complex indices than statistical downscaling has yet to be investigated. In the absence of such research, we assume a similar reduction in skill for complex indices in this section compared with simpler ones. Also, data requirements further reduce our ensemble size in some cases. Finally, each of these indices except WSDI and CSDI are directly affected by RCM historical bias, unlike those in the preceding sections. For all these reasons, interpretation of results in this section require additional caution.

The percentage increases at individual grid boxes for some of the variables below can be large (Table 7) when few cases occurred in the historical run (i.e., WSDI, CSDI, R20mm, SU, and GSL). For SU and GSL, there was at least one grid box with no occurrences in the past and at least one occurrence in future, which results in infinity for maximum change.

Consecutive days CLIMDEX indices

- WSDI: warm spell duration index
- CSDI: cold spell duration index
- CDD: maximum length of dry spell
- CWD: maximum length of wet spell

The warm spell duration index (WSDI) is the annual count of days with at least 6 consecutive days with daytime high temperature warmer than the 90th percentile from the 1971-2000 baseline. The basin-average historical baseline WSDI varies from 4 to 7 days. Note that a value lower than the minimum 6-day warm spell length indicates that warm spells do not occur in every year during the baseline. The range of projected change in the basin average is a considerable increase of 9 to 40 days, about a 150% to 560% increase at most locations (Table 6), with a maximum increase of over 900%.

The cold spell duration index (CSDI) is analogous to WSDI but for cold days: i.e., the annual count of days with at least 6 consecutive days when the night time low temperature is below the 10th percentile from the 1971-2000 baseline. The basin-average historical baseline CSDI is 3 to 7 days. The same 6-day spell length minimum noted above also applies to cold spells. The basin-average CSDI is projected to decrease by 2 to 4 days below baseline durations.

Maximum length of dry (CDD) and wet (CWD) spell is the maximum number of consecutive days with precipitation < 1mm and >= 1mm, respectively. Projected changes to both CDD and CWD are small, generally less than 10%. Grid boxes where wet spells are projected to increase are generally also projected to experience more dry spells according to all runs but GFDL driven RCM3 run which projects fewer dry spells in areas with more wet spells. Overall, slightly more locations are projected to experience increases than decreases in both wet and dry spells. Since these are both annual measures, it is not clear whether these projected changes reflect increases in wet season wet spells and dry season dry spells, or if both increase throughout the year.

Threshold CLIMDEX indices

- GSL: growing season length
- FD: number of frost free days
- SU: number of summer days
- ID: number of icing days
- TR: number of tropical nights
- PRCPTOT: annual total precipitation in wet days
- SDII: simple precipitation intensity index
- R10mm: annual count of days when precipitation >= 10mm
- R20mm: annual count of days when precipitation >= 20mm

Basin-average growing season length (GSL) is projected to increase by 18 to 35 days, with most of the smallest increases in the Northern East Kootenay. This is approximately a 20% to 30% increase from baseline in most locations. Most runs project a decrease of roughly 15% in the number of frost days (FD). A decrease is projected in the number of days when the daytime high is below 0°C (icing days; ID). The projected basin-average ID decrease is 17 to 33 days, or about 10% to 30% below baseline.

An increase is projected by all runs in basin-average days when daytime high temperature >25°C (summer days; SU). At individual grid boxes the changes vary from near zero to an increase of 34 days. SU depends on a fixed threshold and most of the RCMs have a cold bias (Section 2). Although the bias is a factor, large WSDI (a relative index) increases are consistent with the SU increase and together these indices describe a projection for warm spells and warm days becoming a considerably more regular feature of mid-21st century climate. In all but one run, the annual count of days when night time low temperature is greater than 20°C (tropical nights; TR) did not ever occur in the baseline and is also not projected to occur by the 2050s. HRM3 driven by HadCM3, which has a warm bias in the baseline of 2.5°C simulated a basin average of 0.6 nights in the past and an increase by the 2050s of 3.5 days. As HRM3's past bias is comparable to the projected change by the 2050s, this result is an indication that tropical nights could begin to occur in the basin in the latter part of the 21st century.

PRCPTOT is the total precipitation that occurs on wet days (when precipitation >= 1 mm). It is projected to increase in most of the basin according to most runs, although there is considerable disagreement between runs about the amount and pattern of change as with projected total precipitation (Figure 17). The projected basin-average increase ranges from 49 mm to 112 mm, an increase of 6% to 10%, in all runs but GFDL driven RCM3, which projects similar values through all of the basin except the southern half of the two southern sub-regions, where decreases of up to 50% are projected. The SDII is the precipitation *per day* on wet days (when precipitation >= 1 mm). It is projected to increase throughout the basin, according to all models, but generally by less than 10%.

The number of days with precipitation > 10 mm (R10mm) is projected to increase slightly throughout the basin, with the largest increases in Columbia Shuswap according to most runs. The basin-average increase is 1 to 5 days, or +5% to +15% at most locations, and large increases of up to 12 days (+75%) in the Columbia Shuswap sub-region. Most RCM grid boxes in the basin had few days with precipitation > 20 mm (R20mm) in the simulated past, but most runs project increases in future of up to 2 days throughout most of the basin and larger increases of up to 8 days per year in Columbia Shuswap.

Specialized complex indices

See Section 2 for more information on the specialized complex indices. Each depends on at least two thresholds, so these results must be interpreted with great caution.

- Freeze thaw cycles: night-time low < 0°C and day-time high > 0°C
- Rain on frozen ground: precipitation > 6 mm when no snow on ground and temperature < 0°C
- Rain on snow: snow pack > 10 mm, precipitation > 30 mm, and temperature > 0°C
- Rapid snow melt: snow melt > 10 cm

Over the entire basin, the average 1971-2000 daytime high is below freezing in December and January for all runs. Freeze-thaw cycles tend to occur in the shoulder seasons before and after these winter months. Increases in the number of freeze-thaw cycles might be expected if winter warmed enough that events began to occur throughout the coldest months. Decreases might be expected in an even warmer situation where night-time lows were commonly above freezing. While basin-average freeze thaw cycles varied from 17 to 27 per year during the 1971-2000 baseline, there is very little agreement between runs as to patterns or even the direction of change. All runs indicate modest change of at most 5 events per year in either direction, suggesting that the projected warming remains insufficient to substantially affect the frequency of freeze-thaw cycles.

Rain on snow events exhibit no change in five of the eight runs and considerable (but disparate) changes in the other three (CCSM driven MM5I, CCSM driven WRFG, and CGCM3 driven CRCM). This could reflect a need for refinement of the definition, which has a high precipitation threshold. Only four runs met the data requirements for rain on frozen ground. Of those, CCSM driven WRFG and CGCM3 driven CRCM project little change, CCSM driven MM5I projects a large increase throughout the basin and HadCM3 driven HadRM3 projects a large decrease. Only CCSM driven WRFG and CGCM3 driven CRCM simulations have the data required for the computation of rapid snow melt and they project opposite directions of change.

5. Summary

The ability of NARCCAP RCMs to simulate seasonal and annual temperature and precipitation in the Canadian Columbia Basin was documented in Section 3. It was also shown that RCMs provide added value compared to coarse resolution information such as GCMs. However, by looking to RCMs for the benefits of higher resolution, we necessarily add another step in the modeling chain and limit ourselves to a small ensemble of runs; all ranges reported here arise only from an ensemble of eight runs driven by only four different driving GCM runs that are not equally represented. The projected future changes in the four driving GCMs were compared to the larger PCIC30 ensemble (Figures 3, 4, and 5). The effect of dynamical downscaling with RCMs on simulated climate in the basin is shown in Figures 10 to 14. The fact that the RCMs compare favourably with gridded observations (Figures 6 to 9; Table 3) gives some confidence in their use for assessing extremes (Section 3).

Our investigation (Section 4) reveals projections of warmer temperatures (Figure 15), more frequent warm temperature extremes (Figures 18, 19, 21, and 23), and indications of generally wetter conditions (Figures 16, 17, 20, and 22). Results are summarized below for extremes of four types: temperature, precipitation, other more specialized indices, and implications for the extremes of interest requested by the PAG (Section 2). Finally the role of uncertainty is discussed.

5.1. Temperature

Most of the RCMs used here simulate Columbia Basin temperatures with a slight cold temperature bias relative to observations (Figures 6, 7, and 10). However, all of the RCMs capture inter-annual regional temperature variability during historical simulations as shown in the upper panel of Figure 7 and basic statistics in Table 3. Most RCMs improve on the climatology of the NCEP2 reanalysis data even in terms of bias, in part due to the improved representation of topography in RCMs that is possible at their finer resolution (Figure 8).

Changes in temperature indices projected for the 2050s with the eight NARCCAP RCM runs reflect warming in all parts of the Columbia Basin during all seasons. The basin-average annual temperature is projected to increase by 1.8°C to 2.7°C, an amount that is larger than the normal inter-annual variability as represented by standard deviation of annual mean temperature during 1971-2000 which was roughly 1°C. The increases projected by our small ensemble include about 1 to 3 times as many warm days (TX90p) in summer, 2 to 4 times as many warm nights (TN90p) in summer, generally less than half as many cool nights (TN10p) in winter, and 9 to 40 additional days per year during warm spells (WSDI). While caution is required with the exact numbers (see section 5.5 on uncertainty) it is clear that these results describe a 2050s Columbia Basin with considerably warmer conditions than present. This finding is consistent across all of the RCMs.

5.2. Precipitation

Even with improved resolution, the RCMs are unable to fully replicate the complex topography of the basin (Figure 8). The strong orographic effects of mountainous terrain in the basin produce large variations over short distances, with more precipitation observed on windward slopes and less precipitation received on leeward slopes and in valleys. While better captured by RCMs than GCMs, small-scale patterns are still not well represented (Figure 11). Generally, historical agreement of RCMs with observations is relatively lower for precipitation than temperature (e.g., correlation in Table 3) but this is also true of historical agreement between observational datasets (Figures 6 and 7). Projected 2050s change is smaller relative to natural variability for precipitation than temperature. The RCMs reduce precipitation biases compared with their coarse resolution driving data as evident in Figures 6, 7, 9, and 11. The amount of projected change in precipitation differs more among models than between seasons (Figures 16 and 17). Precipitation changes are more spatially variable compared to temperature changes as well, with larger increases projected in the Northern areas of the basin, particularly the Columbia Shuswap sub-region shown in Figure 1. Several runs project decreased precipitation in summer months.

5.3. Other extremes

Some of the more complex variables such as rain on frozen ground, rain on snow, snow depth, and rapid snow melt can only be analyzed using a subset of the RCMs due to data availability limitations. Although these more complex indices more specifically address some impacts of interest, they are also associated with the most uncertainty. These results should be considered preliminary estimates only. Changes are projected in both directions for each of the “specialized indices” described in Section 2.2. See Appendix 3 for a list of potential extensions to this initial investigation of extremes in the Canadian Columbia Basin.

5.4. Indices of interest

The seven categories of indices most relevant to adaptation in the basin as determined by the PAG (Section 2.1 and 2.3) include several that were addressed by the results and discussion (Section 4). Most of the impacts addressed by these categories require further analysis with specific indices or impacts analysis, but some general statements can be made about the findings in this report that are relevant to each of the seven categories.

Drought and extreme fire weather can be expected to increase as a result of slight increases to dry spells (CDD), decreased summer precipitation (RX1day summer), and large increases in warm extremes (TXx, TX90p, return periods). Late spring frosts and ground penetrating frost can be expected to decrease as a result of warming (TNn, TN10p, return periods). High intensity precipitation is projected to increase (RX1day, RX5day, R95pTOT, R99pTOT, R10mm, and R20mm). Extreme stream low flow events would be more likely when increased dry spells (CDD), decreased summer precipitation (RX1day summer), and/or warmer summer temperatures (TXx, TX90p, return periods) result in reduced low flows in summer. However, projected increases in cold season precipitation would be a moderating and competing factor in some watersheds. Where changes in both directions are projected, adaptation planning would ideally plan for change in either direction.

5.5. Uncertainty

As a first investigation into projected changes in extremes, it is hoped that the information provided in this report will be used to inform adaptation projects in the Columbia Basin, in particular the Communities Adaptive to Climate Change Initiative of the Columbia Basin Trust. For this reason, it is important to consider five key differences between the information provided here and that provided in previous regional analyses, each of which that has important implications for describing uncertainty in projected climate change.

1. Limited number of ensemble members: Only eight NARCCAP were available at the time of analysis. Additional runs could change the balance of findings considerably.

Assessments of future projected change from GCMs have typically been based on at least 30 runs from 15 models, and some have used as many as 142 runs from 22 models. Our small ensemble could mean that projected ranges of change are too narrow or are unduly influenced at either end by a run that may eventually turn out to be an outlier when compared to additional runs. In addition, we expect higher variability at higher resolution so the number of ensemble members is even more important for this reason (Li et al. 2012).

2. Uneven distribution of RCMs and driving GCMs: The ensemble is driven by only four different GCM runs and two of those runs provide the driving data for six of the eight members of the ensemble (three each). Similarly, the eight runs are produced with five different RCMs, three of which are driven by two different GCMs and two of which are driven only by a single GCM each. Figures 3 and 4 show that the four driving GCM runs in our ensemble are generally the warmer members of a larger ensemble of GCMs. This indicates that our results may on average be warmer than a wider ensemble. There is not necessarily a direct correspondence between the amounts of warming projected by an RCM and its driving GCM run, however (Figure 13).
3. Emissions scenario and baseline period: All of the RCM simulations here are driven by the A2 emissions scenario, which implies slightly more warming by the 2050s than the lower B1 emissions scenario (Section 4). Conversely, the fact that the baseline period for anomalies is 1971-2000 rather than 1961-1990 would have the opposite effect, though also small (Section 4).
4. Ranges of averages: In this report, we often report regionally-averaged results, particularly for spatially smooth projected changes. These may be compared directly to regionally averaged changes in temperature and precipitation from GCMs subject to the concerns described in the preceding three bullets. In other cases we have reported ranges of differences within sub-regions or at individual grid boxes and some indices are annual aggregates while others include different times of year. A range of changes in regional or annual averages can be considerably different from that derived from individual grid boxes and months (e.g., TXx Section 4.2, Figure 23) and care must be taken to ensure ranges are interpreted with these details in mind.

References

Bürger, G., T. Q. Murdock, A. T. Werner, S. R. Sobie, and A. J. Cannon, 2012: Downscaling Extremes—An Intercomparison of Multiple Statistical Methods for Present Climate. *J. Clim.*, 25, 4366–4388, doi:10.1175/JCLI-D-11-00408.1.

Castlegar, City of, 2011: Adapting to Climate Change Project Summary Report & Action Plan. City of Castlegar, 69. http://www.cbt.org/uploads/pdf/Castlegar_Climate_Change_Adaptation_Report_final.pdf

Goodess, C. M., C. Frei, and J. Schmidli, 2005: Temperature and precipitation extremes at the station and climate model grid-point scales: Some lessons learnt from the statistical and dynamical approaches to downscaling used in the STARDEX project. *Geophysical Research Abstracts*, **7,** 03758.

Hosking, J. R. M. W., J.R Wood, E.F., 1985: Estimation of the generalized extreme-value distribution by the method of probability-weighted moments. *Technometrics*, **27,** pp. 251-261.

IPCC, 2012: Summary for Policymakers. In: *Managing the Risks of Extreme Events and Disasters to Advance Climate Change Adaptation* [Field, C. B.,Barros, V., Stocker, T.F., Qin, D., Dokken, D., Ebi, K.L., Mastrandrea, M. D., Mach, K. J., Plattner, G.-K., Allen, S. K., Tignor, M. and P. M. Midgley (eds.)]. A Special Report of Working Groups I and II of the Intergovernmental Panel on Climate Change. Cambridge University Press, Cambridge, UK, and New York, USA, pp. 1-19.

Kalnay, E., and Coauthors, 1996: The NCEP/NCAR 40-Year Reanalysis Project. *Bulletin of the American Meteorological Society*, **77,** 437-471.

Kendon, E. J., R. G. Jones, E. Kjellström, and J. M. Murphy, 2010: Using and Designing GCM-RCM Ensemble Regional Climate Projections. *Journal of Climate*, **23,** 6485-6503.

Kharin, V. V., and F. W. Zwiers, 2000: Changes in the Extremes in an Ensemble of Transient Climate Simulations with a Coupled Atmosphere-Ocean GCM. *Journal of Climate,* **13,** 3760-3788.

Kharin, V. V., F. W. Zwiers, X. Zhang, and G. C. Hegerl, 2007: Changes in Temperature and Precipitation Extremes in the IPCC Ensemble of Global Coupled Model Simulations. *Journal of Climate*, **20,** 1419-1444.

Kistler, R., and Coauthors, 2001: The NCEP/NCAR 50-year reanalysis. *Bulletin of the American Meteorological Society* **82,** 247.

Klein Tank, A. M. G., F. W. Zwiers, and X. Zhang, 2009: Guidelines on analysis of extremes in a changing climate in support of informed decisions for adaptation, 56 pp.

Lane, O., S. Cohen, and T. Q. Murdock, 2010: Climate Change Impacts and Adaptation in the Canadian Columbia River Basin: A Literature Review.

Li, G. Z., X. Zwiers, F.W.Wen, Q.H., 2011: Quantification of uncertainty in high resolution temperature scenarios for North America. *Journal of Climate*.

McKenney, D. W., J. H. Pedlar, P. Papadopol, and M. F. Hutchinson, 2006: The development of 1901-2000 historical monthly climate models for Canada and the United States. *Agricultural and Forest Meteorology*, **138,** 69-81.

Meehl, G.A., T.F. Stocker, W.D. Collins, P. Friedlingstein, A.T. Gaye, J.M. Gregory, A. Kitoh, R. Knutti, J.M. Murphy, A. Noda, S.C.B. Raper, I.G. Watterson, A.J. Weaver and Z.-C. Zhao, 2007: Global Climate Projections. In: Climate Change 2007: The Physical Science Basis. Contribution of Working Group I to the Fourth Assessment Report of the Intergovernmental Panel on Climate Change [Solomon, S., D. Qin, M. Manning, Z. Chen, M. Marquis, K.B. Averyt, M. Tignor and H.L. Miller (eds.)]. Cambridge University Press, Cambridge, United Kingdom and New York, NY, USA.

Mesinger, F., and Coauthors, 2005: North American Regional Reanalysis: A long-term, consistent, high-resolution climate dataset for the North American domain, as a major improvement upon the earlier global reanalysis datasets in both resolution and accuracy. *Bulletin of the American Meteorological Society*, **87,** 343.

Mitchell, T. D., and P. D. Jones, 2005: An improved method of constructing a database of monthly climate observations and associated high-resolution grids. *International Journal of Climatology,* **25,** 693-712.

Murdock, T. Q., and A. T. Werner, 2011: Canadian Columbia Basin Climate Trends and Projections: 2007-2010 Update, 43 pp.

Murdock, T. Q., J. Fraser, and C. Pearce, 2007: Preliminary Analysis of Climate Variability and Change in the Canadian Columbia River Basin: Focus on Water Resources 2006. Report, 57 pp.
Panofsky, H. A., and G. W. Brier, 1958: *Some applications of statistics to meteorology.* The Pennsylvania State University.

Pearce, C., 2011: Climate Change in the Canadian Columbia Basin: Continuing the Dialogue, 22 pp.
Peterson, T. C., C. Folland, G. Gruza, W. Hogg, A. Mokssit, and N. Plummer, 2001: Report on the Activities of the Working Group on Climate Change Detection and Related Rapporteurs 1998-2001, 143 pp.

Rodenhuis, D., K. Bennett, A. Werner, T. Q. Murdock, and D. Bronaugh, 2009: Hydro-climatology and Future Climate Impacts in British Columbia, revised 2009, 132 pp.

van den Brink, H. W., and G. P. Können, 2011: Estimating 10000-year return values from short time series. *International Journal of Climatology*, **31,** 115-126.

van der Kamp, D. W., and G. Bürger, 2011: Future projections of fire weather severity in southeast British Columbia using statistical downscaling, 30 pp. Pacific Climate Impacts Consortium project report.

van der Kamp, D. W., G. Bürger, and T. Q. Murdock, 2011: Future projections of drought indices in southeast British Columbia using statistical downscaling, 27 pp. Pacific Climate Impacts Consortium project report.

Zhang, X., F. Zwiers, and T. Peterson, 2008: The adaptation imperative: is climate science ready? . *World Meteorological Organization Bulletin*, **57,** 6.

Zhang, X., L. A. Vincent, W. D. Hogg, and A. Niitsoo, 2000: Temperature and precipitation trends in Canada during the 20th Century. *Atmosphere-Ocean*, **38,** 395-429.

Zhang, X., and Coauthors, 2011: Indices for Monitoring Changes in Extremes Based on Daily

Temperature and Precipitation Data. *Wiley Interdisciplinary Reviews: Climate Change, 2*(6), 851–870. doi:10.1002/wcc.147

Zwiers, F. W., M. A. Schnorbus, and G. D. Maruszeczka, 2011: Hydrologic Impacts of Climate Change on BC Water Resources: Summary Report for the Campbell, Columbia and Peace River Watersheds, 17 pp.

Appendix 1: Results summary tables

Table 5: Summary of projected changes for all individual grid boxes from all eight runs and all months for variables except those that are only annual (see Table 6). In addition to minimum, median, and maximum values, the 10th, 25th, 75th, and 90th percentiles of all changes are shown. See Section 2 for definitions of indices.

Index	Units	Min	10	25	50	75	90	Max
P	mm/year	-671	-108	-26	51	133	243	1616
P	%	-50	-12	-3	6	16	26	102
T	°C	0.4	1.3	1.7	2.2	2.8	3.4	5.1
TXx	°C	-0.4	0.7	1.3	1.9	2.8	3.6	11.7
TNx	°C	-0.3	0.9	1.4	2.0	2.5	3.0	6.4
TXn	°C	-5.4	0.8	1.4	2.2	3.1	3.9	6.8
TNn	°C	-3.1	1.3	2.0	2.9	4.0	5.1	10.6
TN10p	Ratio	0.0	0.1	0.2	0.4	0.5	0.6	1.2
TX10p	Ratio	0.0	0.2	0.3	0.4	0.6	0.7	1.2
TN90p	Ratio	0.8	1.5	1.8	2.2	2.7	3.3	6.1
TX90p	Ratio	0.6	1.2	1.5	1.9	2.4	2.9	5.7
DTR	°C	-6.5	-1.4	-0.8	-0.5	-0.1	0.4	4.1
RX1day	mm	-13	-2	0	1	3	4	19
RX5day	mm	-20	-3	-1	2	5	8	39
RX1day	%	-55	-10	-1	8	18	29	141
RX5day	%	-49	-10	-2	6	16	25	98

Table 6: Summary of projected annual changes for all individual grid boxes from all eight runs. In addition to minimum, median, and maximum values, the 10th, 25th, 75th, and 90th percentiles of all changes are shown. See Section 2 for definitions of indices.

Index	Units	Min	10	25	50	75	90	Max
P	mm	-56	7	30	54	92	137	353
P	%	-6	1	4	6	9	12	20
T	°C	1.7	1.8	2.1	2.3	2.5	2.7	3.1
FD	Days	-49	-42	-37	-33	-29	-18	-14
SU	Days	0	0	1	4	11	22	34
ID	Days	-41	-34	-31	-27	-22	-18	-10
TR	Days	0	0	0	0	0	0	19
GSL	Days	7	17	21	27	34	47	75
TXx	°C	1.0	1.3	1.6	2.0	2.4	2.6	3.3
TNx	°C	1.1	1.4	1.6	1.9	2.3	2.4	2.9
TXn	°C	1.1	1.5	1.8	2.2	2.6	2.8	3.4
TNn	°C	2.0	2.4	2.5	2.8	3.3	3.8	4.5
TN10p	Ratio	0.2	0.3	0.3	0.4	0.4	0.4	0.5
TX10p	Ratio	0.3	0.4	0.4	0.4	0.5	0.5	0.6
TN90p	Ratio	1.8	1.9	2.1	2.4	2.6	2.7	3.2
TX90p	Ratio	1.5	1.7	1.8	2.0	2.1	2.4	3.0
WSDI	Days	4	8	10	17	24	35	52
CSDI	Days	-6	-4	-3	-3	-2	-1	0
DTR	°C	-1.5	-1.0	-0.7	-0.4	-0.2	0.0	0.2
SDII	mm	-0.2	0.1	0.2	0.3	0.5	0.7	1.4
R10mm	Days	-3	0	1	3	5	7	12
R20mm	Days	-1	0	0	1	2	3	8
CDD	Days	-17	-2	-1	0	1	3	12
CWD	Days	-4	-1	0	0	1	2	5
R95pTOT	mm	-25	5	18	42	72	101	232
R99pTOT	mm	-33	-4	5	19	34	49	128
PRCPTOT	mm	-54	7	30	53	91	138	353

Table 7: Summary of projected annual changes for all individual grid boxes from all eight runs for variables that can be expressed as percent of baseline. In addition to minimum, median, and maximum values, the 10th, 25th, 75th, and 90th percentiles of all changes are shown. See Section 2 for definitions of indices.

Index	Units	Min	10	25	50	75	90	Max
FD	%	-26	-19	-16	-12	-11	-7	-5
SU	%	-100	40	69	166	527	1600	∞
ID	%	-49	-34	-28	-21	-15	-11	-7
GSL	%	7	13	16	22	54	177	∞
WSDI	%	63	150	200	311	431	559	913
CSDI	%	-100	-83	-75	-63	-52	-40	20
SDII	%	-2	2	4	6	9	11	16
R10mm	%	-13	2	8	13	21	29	75
R20mm	%	-57	-3	10	24	44	68	600
CDD	%	-23	-11	-5	1	8	17	63
CWD	%	-23	-8	-3	2	9	14	26
R95pTOT	% of P	-1	2	4	6	7	8	13
R99pTOT	% of P	-2	0	2	2	4	4	9
PRCPTOT	% of P	-6	1	4	6	10	12	19

Table 8: Summary of projected change in ratio of future frequency of return period to historical frequency, for 5-, 10-, and 25-year return periods for all individual grid boxes from all eight runs. In addition to minimum, median, and maximum values, the 10th, 25th, 75th, and 90th percentiles of all changes are shown. See Section 2 for more information about return period analysis.

Variable	Period	Min	10	25	50	75	90	Max
Daily Temperature – Cold Side	5	0.0	0.1	0.2	0.3	0.5	0.6	0.9
	10	0.0	0.0	0.1	0.3	0.4	0.6	0.9
	25	0.0	0.0	0.1	0.3	0.5	0.6	1.3
Daily Temperature – Warm Side	5	1.0	1.6	2.1	2.9	3.7	4.0	4.5
	10	1.0	1.5	2.3	3.8	5.8	6.6	8.0
	25	0.3	1.4	2.6	5.1	9.9	12.5	17.3
Daily Precipitation	5	0.0	0.7	1.0	1.4	1.8	2.3	3.6
	10	0.0	0.6	0.9	1.4	2.2	2.8	6.1
	25	0.0	0.3	0.8	1.5	2.8	4.1	12.1
3-hourly Precipitation	5	0.2	0.9	1.2	1.5	2.1	2.5	3.9
	10	0.0	0.7	1.1	1.7	2.5	3.3	6.8
	25	0.0	0.3	0.9	2.0	3.4	5.0	14.4

Table 9: Summary of projected change in ratio of future frequency of return period to historical frequency, for lower bounds of 5-, 10-, and 25-year return periods for all individual grid boxes from all eight runs. In addition to minimum, median, and maximum values, the 10th, 25th, 75th, and 90th percentiles of all changes are shown. See Section 2 for more information about return period analysis.

Variable	Period	Min	10	25	50	75	90	Max
Daily Temperature – Cold Side	5	0.0	0.1	0.2	0.3	0.4	0.5	0.6
	10	0.0	0.0	0.1	0.2	0.2	0.3	0.6
	25	0.0	0.0	0.0	0.0	0.1	0.1	0.2
Daily Temperature – Warm Side	5	0.3	0.8	1.1	1.9	2.8	3.3	3.9
	10	0.0	0.4	0.8	1.9	3.8	4.6	6.7
	25	0.0	0.1	0.7	2.4	5.7	7.7	11.7
Daily Precipitation	5	0.0	0.5	0.6	0.7	0.7	0.8	0.9
	10	0.0	0.1	0.2	0.4	0.5	0.6	0.9
	25	0.0	0.0	0.0	0.1	0.3	0.4	0.7
3-hourly Precipitation	5	0.1	0.4	0.5	0.6	0.7	0.7	1.0
	10	0.0	0.0	0.1	0.2	0.3	0.4	0.9
	25	0.0	0.0	0.0	0.0	0.1	0.2	0.9

Table 10: Summary of projected change in ratio of future frequency of return period to historical frequency, for upper bounds of 5-, 10-, and 25-year return periods for all individual grid boxes from all eight runs. In addition to minimum, median, and maximum values, the 10th, 25th, 75th, and 90th percentiles of all changes are shown. See Section 2 for more information about return period analysis.

Variable	Period	Min	10	25	50	75	90	Max
Daily Temperature – Cold Side	5	1.4	1.6	1.7	1.8	1.9	2.1	2.7
	10	1.5	1.9	2.0	2.2	2.4	2.6	3.9
	25	2.0	2.5	2.7	3.0	3.3	3.9	7.2
Daily Temperature – Warm Side	5	1.8	2.5	3.0	3.8	4.4	4.7	5.0
	10	2.0	2.9	3.9	5.6	7.5	8.2	9.4
	25	1.5	3.5	5.4	8.9	14.7	17.0	21.4
Daily Precipitation	5	1.1	1.2	1.2	1.4	1.8	2.3	4.7
	10	1.1	1.4	1.5	1.6	2.2	2.8	9.1
	25	1.3	1.7	2.1	2.4	2.9	4.1	21.9
3-hourly Precipitation	5	1.0	1.2	1.3	1.5	2.1	2.5	3.9
	10	1.1	1.5	1.7	1.9	2.5	3.3	6.8
	25	1.1	2.1	2.4	2.8	3.5	5.0	14.4

Appendix 2: Table of RCM details

Table 11: Major characteristics of RCMs in NARCCAP

Model	Dynamics	Lateral Boundary Treatment	Land Surface	TWL *	Vege-tation Types	Boundary Layer	Explicit Moist Physics	Cumulus Parameter-ization
CRCM 4.2@	Nonhydro-static, Compress-ible	9 points spectral *nudging* of horizontal wind	CLASS 2.7	3/3	21	Local K, gradient Richardson number formulation	Removal of super-saturation	Mass flux
PRECIS	Hydro-static, Incom-pressible	4 points (Davies and Turner method)	MOSES	4/4	53	First order turbulent mixing	Prognostic cloud liquid and ice; liquid potential temperature	Mass flux, including downdraft
MM5	Nonhydro-static, Compress-ible	4 points (linear relaxation)	NOAH	4/4	16	Hong-Pan (MRF) countergradi ent, non-local K	Dudhia simple ice	Kain-Fritsch2 mass flux
RegCM3	Hydro-static, Compress-ible	12 points (expo-nential relaxation)	BATS	1/3	19	Non-local K, countergradi ent flux	SUBEX, prognostic cloud water	Grell with Fritsch-Chappell closure
ECPC RSM@	Hydro-static, Incom-pressible	Pertur-bations relaxed at boundaries; *spectral filter*	NOAH	4/4	13	Hong-Pan non-local K	Removal of super-saturation	Simplified Arawaka-Schubert
WRF	Nonhydro-static, Compress-ible	15 grid points (expo-nential relaxation)	NOAH	4/4	24	Yonsei Univ. (explicit entrainment)	Prognostic cloud liquid and ice, rain, snow	Kain-Fritsch2 mass flux

*TWL = Thermal / Water Layers

@ = Uses interior nudging

Appendix 3: Possible Future Work

Extensions to the work carried out under this project that could provide valuable additional information include:

1. Assess historical trends in indices of extremes
2. Investigate capability of RCMs to simulate indices of extremes over the historical period
3. Re-evaluate projected changes using bias-correction, threshold scaling, or statistical downscaling
4. Perform threshold scaling and/or statistical downscaling at specific stations
5. Extend analysis in further detail for a smaller number of indices
6. Analyze additional specialized indices
    a. drought
    b. fire weather index
    c. revised complex index definitions
    d. heating, cooling, and growing degree days
7. Re-compute return periods using goodness of fit and feasibility tests (Kharin & Zwiers 2000).
8. Investigate longer (50-, 100-, 200- year) return periods. (For example by regionally aggregating temperature and precipitation to obtain regional return periods as in van den Brink & Können, 2011).
9. Investigate impacts on extremes of stream low and high flow
10. Re-do (parts of) analysis with additional RCM projections as they continue to be made available from NARCCAP and other sources, including higher resolution RCMs
11. Estimate spread that might be induced by other GCMs if they had been available (Kendon et al., 2010)
12. Extend ensemble using empirical relationships between existing GCM-RCM pairs to produce high resolution projections for additional GCM runs (Li et al. 2012).